nature portfolio

Peer Review File

Safe electrolyte design with isolated solvation nanoclusters for high-energy lithium metal batteries

Corresponding Author: Professor Fei Du

This file contains all reviewer reports in order by version, followed by all author rebuttals in order by version.

Version 0:

Reviewer comments:

Reviewer #1

(Remarks to the Author)
In this paper, the authors introduce a novel electrolyte design strategy using a cyclic hydrofluorocarbon diluent to suppress diluent-ion pair interactions, thereby promoting the formation of uniform solvation nanoclusters. This structural regulation enhances Li+ transport and improves interphase stability. The electrochemical performance and safety validations are particularly compelling, with the fully-charged cell passing nail penetration and overcharge tests. Overall, the work is scientifically rigorous, well executed, and addresses critical safety challenges in lithium metal batteries. However, some conceptual and experimental details are missing and require clarification. Therefore, the manuscript could be accepted by Nature Communications after carefully addressing the following points:
1. The authors used NMR chemical shifts to demonstrate the influence of HFC on Li+, FSI-, and solvents within the solvation structure. Although distinct shifts were observed, their magnitudes are relatively small. Could such chemical shift variations result from experimental error?
2. The authors selected a fixed molar ratio for the electrolyte recipe as 1:1:1.5. The authors should provide additional experiments and discussion on whether this ratio is optimal.
3. The CE of SRCE is 99.6%, which is quite high compared to other references. How many cells were tested, and what is the standard deviation? This information is important for reproducibility.
4. In Figure 5h, ICP-OES shows significantly lower TM dissolution for SRCE. Were the Li anodes also analyzed for TM content? Except for the ICP, did the authors conduct other experiments on TM crossover? This could further confirm the suppression of TM crossover.
5. The SRCE demonstrates good cycling stability at an elevated temperature of 60 ℃, supported by LSV measurements using Li||Al cells. Could leakage current tests and other tests on Li||NCM811 cells at elevated temperatures be provided to further validate interfacial stability?
6. Some experimental details are missing. How was the lithium-ion diffusion coefficient in Figure 2g measured? How were the quantitative NMR results in Figure 5i calculated? What are the assembly details for the 6 Ah pouch cells, and is the energy density based on total cell mass or active materials only?

Reviewer #2

(Remarks to the Author)
This paper reports a new electrolyte, sterically regulated high-concentration electrolytes (SHCE), by employing nonflammable fluorinated alkane HFC molecules for Li metal batteries. Owing to their low polarizability, the HFC molecules are suggested to alter the solvation structure, forming the smaller nanoclusters of ion pairs, which is supported by NMR and WAXS characterization. The SHCE electrolyte then shows enhanced cycling performance, which is attributed to improved interfacial stability at both the Li metal anode and NCM cathode, in addition to its excellent safety performance. Overall, the paper is well-written, and the proposed electrolyte demonstrates superior performance based on robust characterization and evaluation. I recommend publication of this work in Nature Communications, but there are several points to be addressed before publication.

1. Regarding the interfacial stability on the Li metal anode side, the authors show the highest C-F signal in the SHCE electrolyte, which should be attributed to the decomposition of HFC diluent molecules. However, in the earlier section, the author proposed that the HFC interacts weakly with both cations and anions, which would minimize the contribution of HFC

to SEI formation. The author should clarify this apparent inconsistency and revise the discussion accordingly. Or it seems that the peak assigned to C-F in the SRCE electrolyte shows a noticeable shift in peak position compared to the others. The author should consider other possible candidates for SEI components in the SRCE electrolyte, or provide a clear explanation for the origin of peak shift.
2. Moreover, it is surprising that the introduction of HFC leads to highly dense and planar Li microstructure. Not only LiF contents, the author should also include the analysis of other critical SEI components, such as Li2O, which might have an impact on such Li morphology, considering that LiF is well known to be mechanically robust.
3. For SEI structure analysis, it is suggested to perform cryo-TEM analysis to show thin and robust CEI as shown in the schematic of Figure 1.
4. In Figure 5i, the authors quantitatively analyzed the remaining amounts of diluents, LiFSI and DME after 200 cycles, but the results appear to be overestimated. If it is true, it would be questionable how those cells can work for prolonged cycles (Figure 4b) even with such large electrolyte loss. Previous work (https://doi.org/10.1038/s41565-025-01935-y) reported that LiFSI consumption is the dominant source of electrolyte loss, whereas the amounts of DME and TTE remain relatively constant. Moreover, in both LHCE and SRCE, diluents are consumed more than DME despite their minimal participation in the solvation sheath and increased oxidation stability. The author should clearly describe the experimental procedure used for the NMR-based quantification and discuss the origin of the apparently large solvent consumption, particularly diluents.
5. In page 6 line 150, HSP distance appears first without its full name.

Reviewer #3

(Remarks to the Author)
The manuscript by Du and coworkers presents a thorough characterization study of a novel localized high concentration electrolyte (LHCE), in which a diluent is added to a concentrated electrolyte to yield two nano-segregated phases, an ion-conducting salt phase and a diluent phase. In particular, the authors' work revolves around the concept that the diluent should distort the lithium solvation shell as weakly as possible. To this purpose, conventional diluents, typically fluorinated ethers, are replaced by a fluorinated cycloalkane which shows weaker interactions with the lithium solvation shell, as demonstrated by NMR and vibrational spectroscopy as well as Density Functional Theory calculations and Molecular Dynamics simulations. The battery cells utilizing this novel electrolyte show superior performance in extensive cell test.

In my opinion, the manuscript could be of interest for Nature Communications if the central design concept would be scrutinized in more detail as detailed below. Otherwise, the study would rather reflect a thorough (and well-done) characterization study of a specific electrolyte formulation, which might be better suited for a more specialized journal. For a prestigeous journal such as Nature, more general takeaway messages and/or design principles that leave a broad impact in the field would be required.

In particlar, the authors' key hypothesis is that the solvation shell is not perturbed in the novel SRCE as compared to the underlying high-concentration electrolyte (HCE), in contrast to an LHCE using the conventional TTE diluent. If this was true, the lithium ion solvation shells in the HCE and the SRCE should be identical and lead to very similar electrolyte decomposition products at the electrode interface. However, experimentally, the authors find different compositions for all three electrolytes (HCE, LHCE and SRCE). Here, I am wondering in how far this contradicts the authors' hypothesis. Of course, I am aware that the transport is improved in the SRCE as compared to the HCE, which likely also affects the interface kinetics. Therefore, it is not entirely clear in how far the observed improved performance of the battery cells arises from the improved transport alone (which would be the case for a standard LHCE as well), the modified SEI/CEI composition, or a combination of both. For example, the transference number of the SRCE is larger than in the LHCE, which could improve cell performance independently from the modified SEI/CEI composition. Would it be possible to disentangle these effects? I believe that the manuscript would benefit if these aspects were discussed in more detail. This would also strengthen statements related to rational electrolyte design such as "Herein, we propose a novel diluent strategy to mitigate the perturbations of solvation structures, including Li+ cations, solvents, and anions."

When discussing a novel rational design principle, I believe that another aspect needs to be mentioned as well: Of course, the diluent should not interfere with the solvation structure. However, if a diluent would interact very weakly with the components of the conducting salt phase, macroscopic phase separation would occur. Therefore, some balancing interaction must be preserved. Could the authors comment on the type of interaction that renders the present SRCE miscible?

Further comments:

- Figures 2a,b & S1 give insights into the interaction strength between Li+ and DME as well as Li+ and the diluent, the interaction between DME and the diluent is shown in Figure S6. Because the weakened interaction between diluent and anions in the SRCE is central to the manuscript, I was wondering if additional DFT calculations between FSI- and TTE as well as HFC could provide further evidence.

- Figure S4: Although it is somewhat obvious, the color coding used in the snapshots should be mentioned in the figure caption. Furthermore, I believe that a table with the coordination numbers in the first shell derived from Figure 4d-f would be helpful. This would support statements such as "Consistent with the NMR and MD simulation results, the addition of TTE has a negligible effect on the coordination number of Li+-FSI- pairs but weakens the inter-CIPs' correlation through strong anion-diluent interactions, resulting in a reduction in both the size and population of nanoclusters.", which is otherwise hard

to judge.

- Line 150: Abbreviation HSP is not introduced at this point.

Version 1:

Reviewer comments:

Reviewer #1

(Remarks to the Author)
After reviewing the revised manuscript, I recommend publishing it in its current form.

Reviewer #2

(Remarks to the Author)
I have carefully reviewed the author's response to my previous comments and the revised manuscript. The author has effectively addressed all of my concerns. The clarifications and additional experiments demonstrate a clear effort to improve the quality and clarity of the work.
Therefore, I recommend the manuscript to be published in Nature Communications in its present form.

Reviewer #3

(Remarks to the Author)
The authors thoroughly addressed my previous remarks and performed additional analyses. In particular, statements on the impact of the novel HFC diluent on the lithium ion solvation shell have been phrased more carefully. In my opinion, the manuscript could be published now.

Response Letter to Reviewers

Reviewer #1:

In this paper, the authors introduce a novel electrolyte design strategy using a cyclic hydrofluorocarbon diluent to suppress diluent-ion pair interactions, thereby promoting the formation of uniform solvation nanoclusters. This structural regulation enhances Li^+ transport and improves interphase stability. The electrochemical performance and safety validations are particularly compelling, with the fully-charged cell passing nail penetration and overcharge tests. Overall, the work is scientifically rigorous, well executed, and addresses critical safety challenges in lithium metal batteries. However, some conceptual and experimental details are missing and require clarification. Therefore, the manuscript could be accepted by Nature Communications after carefully addressing the following points:

Response: We thank the reviewer for the positive comments. We have incorporated additional experiments and analyses in response to the reviewer's suggestions. Our point-to-point replies to the comments are detailed as follows.

1. The authors used NMR chemical shifts to demonstrate the influence of HFC on Li^+, FSI^-, and solvents within the solvation structure. Although distinct shifts were observed, their magnitudes are relatively small. Could such chemical shift variations result from experimental error?

Response: We sincerely appreciate the reviewer's valuable suggestion. For NMR measurements, we applied external references to ensure the accuracy of chemical shifts while maintaining the invariance of the internal solvation environment. Therefore, although the observed chemical shifts are small, they reveal real differences in solvation interactions.

As shown in **Figure R1a**, we employed a coaxial NMR tube configuration (inner tube containing the external reference solution, outer tube containing the test electrolytes). This configuration completely avoids direct contact between the electrolyte and deuterated solvents, thereby preserving the native solvation structure without perturbation. Furthermore, the external references locked in the inner tube could ensure absolute chemical shift accuracy and eliminate baseline drift, measured on a high-resolution Bruker AVANCE III 600 MHz

spectrometer. Therefore, 1 M $Zn(OTf)_2$ in D_2O (-78.84 ppm), 1 M LiCl in D_2O (0 ppm), and D_2O (0 ppm) were adopted as external reference electrolytes for ^{19}F NMR, ^{7}Li NMR, and ^{17}O NMR, respectively (**Figure R1b-e**). With this setup, we observed distinct and reproducible chemical shift differences among the three electrolytes (HCE, LHCE, and SRCE), reflecting genuine diluent-induced changes in the chemical microenvironment.

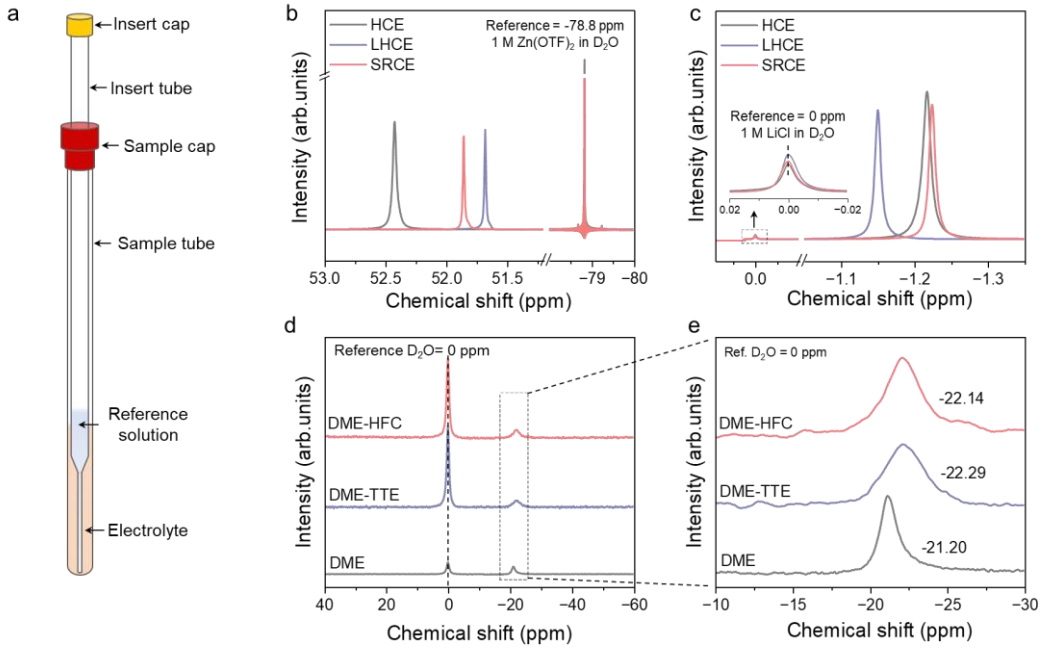

Figure R1. (a) Schematic illustration of the coaxial NMR tube configuration. (b) ^{19}F NMR spectra of FSI^- in three electrolytes, with the external reference signal at -78.84 ppm for comparison (1 M $Zn(OTf)_2$ in D_2O). (c) ^{7}Li NMR spectra of the three electrolytes, referenced to 1 M LiCl in D_2O at 0 ppm. (d-e) ^{17}O NMR spectra of DME and its mixtures with TTE and HFC (external reference: D_2O at 0 ppm), with expanded views highlighting subtle.

Revised Manuscript

"*The solvation structures of the electrolytes were characterized by NMR spectroscopy on a Bruker AVANCE III 600 MHz instrument. To maintain the native solvation environment without perturbation, the coaxial NMR tube configuration was used with the external reference in the inner tube and test electrolytes in the outer tube (**Supplementary Figure 45**). This configuration could ensure the absolute chemical shift accuracy and eliminate baseline drift. External references were 1 M $Zn(OTf)_2$ in D_2O (-78.84 ppm) for ^{19}F NMR, 1 M LiCl in D_2O (0 ppm) for ^{7}Li NMR, and D_2O (0 ppm) for ^{17}O NMR.*" (**Page 21**, **Line 498**)

2. The authors selected a fixed molar ratio for the electrolyte recipe as 1:1:1.5. The authors should provide additional experiments and discussion on whether this ratio is optimal.

Response: We thank the reviewer for this highly constructive comment. We agree that the optimization of the electrolyte formulation should be provided. Our two-stage optimization first fixes the salt-solvent ratio and then optimizes the electrolyte-diluent ratios.

Firstly, the recent literature and our quantitative NMR analysis demonstrate that irreversible consumption of Li salts drives electrolyte depletion and capacity degradation over long-term cycling[1]. Therefore, to extend cycle life, we maximized the initial LiFSI inventory by fixing the salt-to-solvent molar ratio at 1:1, near the solubility limit of LiFSI in DME at room temperature[2], thereby ensuring high salt retention during prolonged cycling. Secondly, by determining the salt-solvent ratio, we systematically varied the diluent (HFC) content to balance ionic transport, Li plating/stripping reversibility, and cathode stability. A series of electrolytes with LiFSI: DME: HFC molar ratios of 1:1:1, 1:1:1.5, 1:1:3, and 1:1:4 (the last requiring heating to be mixable) was investigated. As the HFC content increases from 0 to 1.5, the noticeably enhanced ionic conductivity and Li plating/stripping Coulombic efficiency (CE) indicate the HFC diluents effectively disperse the massive, polymer-like, concentrated networks into isolated nanoclusters, thereby lowering the system's viscosity and promoting fast Li^+ transport kinetics (**Figure R2a-b**). Nevertheless, as the HFC content increases to 4, the ionic conductivity and CE drop to 1.94 mS cm^{-1} and 99.58%, respectively, indicating that the relatively lower Li^+ concentration could support efficient Li^+ migration. At the same time, we conducted a comprehensive evaluation of different HFC ratios based on the cycle life of 2.5 mAh cm^{-2} NCM811||50 μm Li metal full cells, in which the 1:1:1.5 ratio displays a prolonged cycling life (**Figure R2c**). Consequently, the 1:1:1.5 composition offers the best balance of cost and Li^+ reservoir, the highest conductivity (2.88 mS cm^{-1}), the highest reversibility (99.61%), and the best full-cell cycling performance, which was selected as the optimal electrolyte.

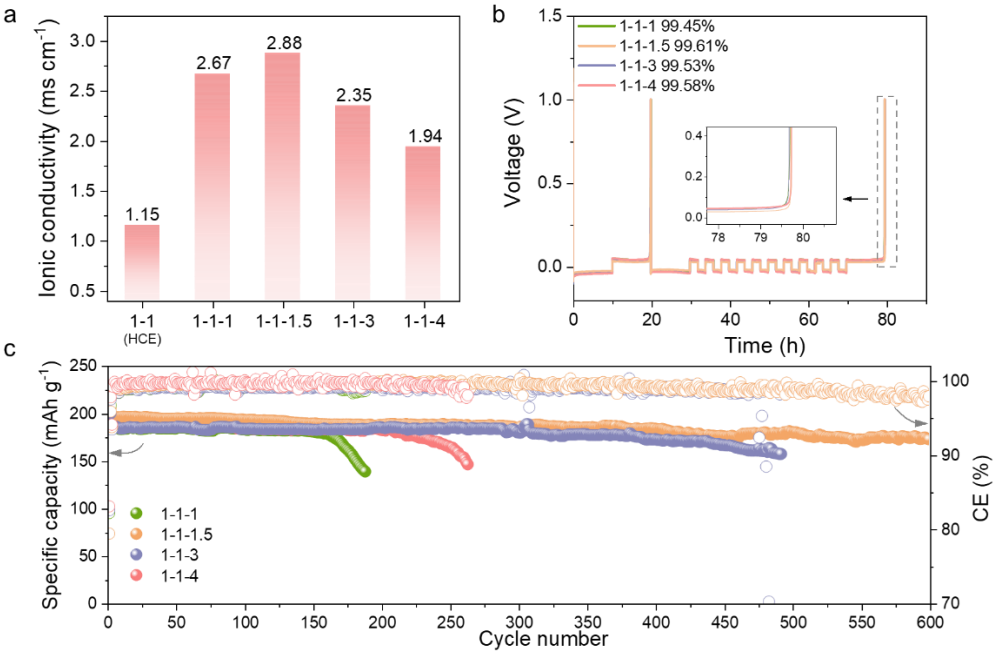

Figure R2. (a) Comparison of ionic conductivities for different electrolyte formulations (*x-y-z* represents the molar ratio of LiFSI: DME: HFC). (b) Comparison of Li plating/stripping CE of Li||Cu cells. (c) Long-term cycling stability of 2.5 mAh cm^{-2} NCM811|| 50μm Li metal full cells in different electrolytes.

Revised Manuscript

"*This composition was selected as the optimal electrolyte, offering the best balance of cost and* Li^+ *reservoir, the highest conductivity, the highest reversibility, and the best full-cell cycling performance (**Supplementary Figure 44**). All mixtures were stirred until homogeneous and allowed to equilibrate before use.*" (**Page 20**, **Line 454**)

3. The CE of SRCE is 99.6%, which is quite high compared to other references. How many cells were tested, and what is the standard deviation? This information is important for reproducibility.

Response: We thank the reviewer for requesting statistical information on the Li plating/stripping Coulombic efficiency (CE) of SRCE. The CE is the average of 5 trials, with a standard deviation of ±0.04% (n=5).

To ensure reproducibility, we tested five independent Li||Cu cells under identical conditions using the modified Aurbach method described in the **Methods** section. The

measured CE values for SRCE are: 99.67%, 99.61%, 99.60%, 99.56%, and 99.59% (**Figure R3**). The average CE is 99.61% with a standard deviation of ±0.04% (n= 5). Among these, we selected trial 2, with a CE of 99.61%, as the representative galvanostatic charge-discharge potential profile for CE of SRCE. These results demonstrate that SRCE consistently delivers high CEs with excellent reproducibility.

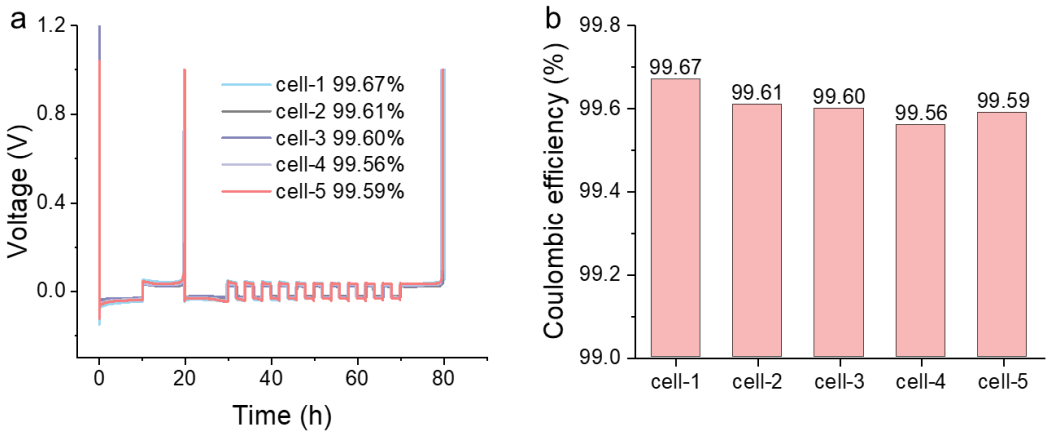

Figure R3. (a) Statistical reproducibility of Li plating/stripping Coulombic efficiency in the SRCE electrolyte. (b) Summary of the corresponding CE values derived from the five individual cells.

Revised Manuscript

"*The modified Aurbach method reveals that SRCE possesses the highest Li plating/stripping Coulombic efficiency (CE) of 99.61% at 25°C (average of 5 trials with standard deviation of ±0.04%), thereby favoring the long-term cycling stability of LMBs (**Figure 3a**).*" (**Page 8**, **Line 184**)

"*The CEs of Li||Cu cells were evaluated using a modified Aurbach method, in which the CE was calculated as the average of 5 trials*." (**Page 20**, **Line 466**)

4. In Figure 5h, ICP-OES shows significantly lower TM dissolution for SRCE. Were the Li anodes also analyzed for TM content? Except for the ICP, did the authors conduct other experiments on TM crossover? This could further confirm the suppression of TM crossover.

Response: We thank the reviewer for this constructive suggestion. The ICP-OES measurement of TM content includes the anode and electrolyte. We have further conducted scanning electron microscope (SEM) with Energy Dispersive X-ray Spectroscopy (EDS) to further confirm the

suppression of TM crossover.

The detailed ICP-OES prepared procedure is as follows (**Figure R4a**). Firstly, after disassembling the cycled cell in an Ar-filled glovebox, the NCM811 cathodes were rinsed with DME, followed by immersion of remaining battery components, including the separator, spacer, case, and spring, in 5 mL of DME for 24 hours to extract transition metals (TMs) from the residual electrolyte. Secondly, the above wash liquid was evaporated at 80 °C in a fume hood, and the resulting residue was dissolved in 2 g H_2O and 1 g nitric acid. At the same time, the Li anodes were removed from the wash liquid and air-oxidized for 48 hours for safe handling. Then the chips were digested in 7 g H_2O and 1g nitric acid to extract the TM deposited on the Li metal surface. Finally, these two digestion solutions, one containing TMs from the electrolyte and surface adsorption, and the other containing TMs deposited on Li metal anodes, were combined and filtered for ICP-OES analysis. Therefore, the reported concentrations reflect the complete inventory of TMs that migrated from the cathode.

Furthermore, we have conducted SEM-EDS to provide direct evidence of TM deposition on Li metal anodes. As shown in **Figure R4b-g**, the EDS results clearly demonstrate that the SRCE electrolyte effectively minimizes TM crossover and deposition on the Li surface, below the detection limit, corroborating our quantitative ICP-OES results.

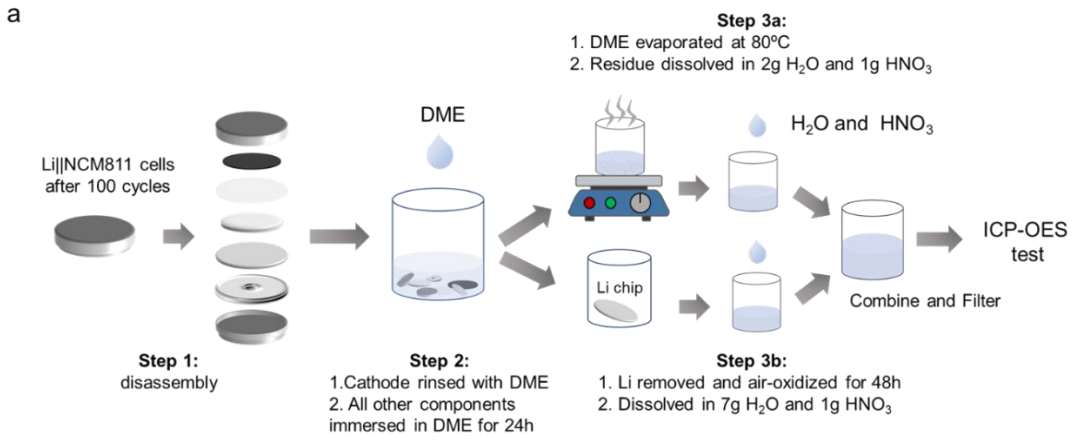

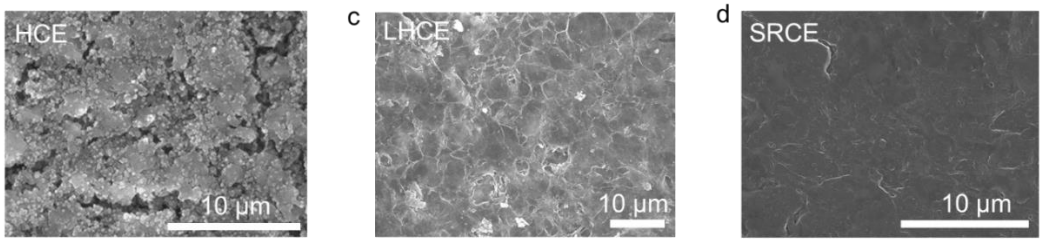

e

Element	At. No.	Mass Norm. [%]	Atom [%]
O	8	22.33	32.12
F	9	21.39	25.92
S	16	54.48	39.11
C	12	1.41	2.69
Mn	25	0.13	0.05
Co	27	0.05	0.02
Ni	28	0.22	0.08

f

Element	At. No.	Mass Norm. [%]	Atom [%]
O	8	28.76	42.46
F	9	9.00	11.19
S	16	61.39	45.22
C	12	0.51	1.00
Mn	25	0.11	0.55
Co	27	0.23	0.09
Ni	28	0.00	0.00

g

Element	At. No.	Mass Norm. [%]	Atom [%]
O	8	36.75	50.84
F	9	8.99	10.48
S	16	53.19	36.71
C	12	1.07	1.97
Mn	25	0.00	0.00
Co	27	0.00	0.00
Ni	28	0.00	0.00

Figure R4. (a) ICP-OES Sample Preparation Workflow. The SEM images and their corresponding EDS spectra of the Li metal after 100 cycles in Li||NCM811 full cells with (b, e) HCE, (c, f) LHCE, and (d, g) SRCE, respectively.

Revised Manuscript:

"*ICP-OES (Agilent 725) was used to determine the dissolution of transition metals in the cathode material of a 2.5 mAh cm^{-2} NCM811||Li cell after 100 cycles* ***(Supplementary Figure 47)****. To accurately determine the respective concentrations of individual transition metals (Ni, Co, Mn) retained in the residual electrolyte and deposited on the Li anode, the cycled cell was disassembled in an argon-filled glovebox. The cathode chip was rinsed with 5 mL of DME, and the washings were collected. The remaining battery components, including the separator, lithium foil, spacer, contact spring, and cathode and anode shells, were immersed in the same wash liquid for 24 hours. The Li chip was subsequently removed and air-oxidized for 48 h. The wash liquid was evaporated at 80 °C in a fume hood, and the resulting residue was dissolved*

in 2 g H_2O and 1 g nitric acid. The oxidized Li metal was separately dissolved in a mixture of 7 g H_2O and 1 g nitric acid. Finally, these two digestion solutions, containing TMs from the electrolyte and surface adsorption and containing TMs deposited on Li metal anodes, were combined and filtered for ICP-OES analysis." (**Page 23**, **Line 561**)

5. The SRCE demonstrates good cycling stability at an elevated temperature of 60 °C, supported by LSV measurements using Li||Al cells. Could leakage current tests and other tests on Li||NCM811 cells at elevated temperatures be provided to further validate interfacial stability?

Response: We thank the reviewer for the insightful suggestion. To further validate the interfacial stability of SRCE at elevated temperature, we have performed additional experiments at 60°C, including CE, LSV, and leaking current.

For Li metal anodes, the Li plating/stripping CE at 60°C are 99.51%, 99.40%, and 99.31% in HCE, LHCE, and SRCE, respectively, demonstrating the reductive stability of the SRCE at elevated temperature (**Figure R5a**). The LSV curves of the Li||Al cells at 60 °C show that the electrolyte oxidation onset potential of SRCE is over 4.3 V, significantly outperforming HCE and LHCE, indicating that the SRCE electrolyte remains robust under thermal stress (**Figure R5b**). To assess long-term interfacial stability under operating conditions, we further conducted high-temperature leakage current measurements on Li||NCM811 cells at 4.3 V. The SRCE cell exhibits rapid current decay, and the current stabilizes at ~1.1 μA, whereas HCE and LHCE show much higher leakage currents of ~4.1 μA and ~56 μA, respectively (**Figure R5c**). These results collectively indicate that the interphase formed in SRCE effectively passivates both electrodes and suppresses parasitic reactions even at elevated temperature, supporting the enhanced full cell cycling stability at 60 °C.

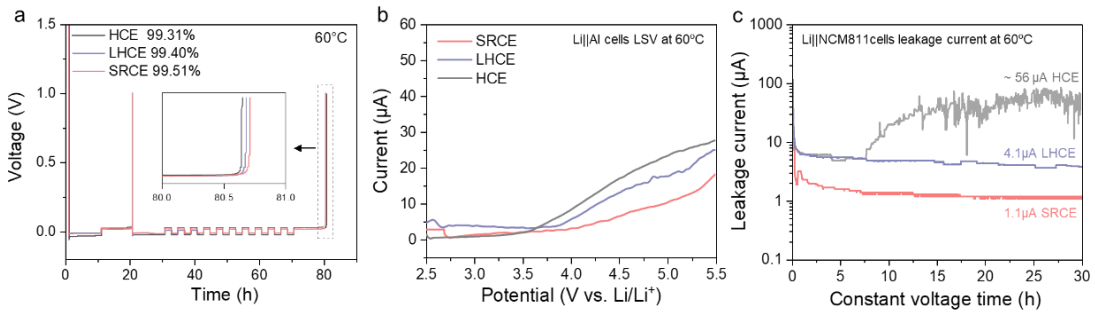

Figure R5. (a) Li plating/stripping CE at 60 °C, measured using the modified Aurbach method.

(b) Linear sweep voltammetry curves of Li||Al cells measured at 0.5 mV s^{-1} at 60 °C. (c) Leakage current profiles of Li||NCM811 cells at 60 °C, holding at 4.3 V for 30 h.

Revised Manuscript:

"*In contrast, SRCE retains 80% capacity after 380 cycles with higher stability for both electrodes, demonstrating its superior thermal resilience and effectively interphase passivation against high-temperature degradation* ***(Supplementary Figure 34).***" (**Page 16, Line 364**)

6. Some experimental details are missing. How was the lithium-ion diffusion coefficient in Figure 2g measured? How were the quantitative NMR results in Figure 5i calculated? What are the assembly details for the 6 Ah pouch cells, and is the energy density based on total cell mass or active materials only?

Response: We thank the reviewer for the thoughtful question regarding the experimental details.

We performed pulsed-field gradient NMR (PFG-NMR) to quantitatively evaluate the self-diffusion coefficients of Li^+ (D_{Li^+}) in the three electrolytes. By measuring the ^7Li NMR spectra under different pulse fields **(Figure R6a-c**), the signal attenuation curves were fitted using the Stejskal-Tanner equation:

$$\ln\left(\frac{S}{S_0}\right) = -\gamma^2 g^2 \delta^2 D(\Delta - \frac{\delta}{3})$$

where δ is the gyromagnetic ratio, g is the gradient strength, and D is the diffusion coefficient.

For the quantitative NMR analysis of electrolyte consumption, the following experimental and calculation procedures were used. The electrolyte mass for 2.5 mAh cm^{-2} NMC811||50 μm Li full cell assembly was precisely recorded for each cell. The full cell was disassembled in an Ar-filled glovebox after 200 cycles, where all components (cathode, anode, separator, spacer, and case) were directly immersed in 2 mL of DMSO-d_6 for 12 h to extract the remaining electrolyte. For subsequent quantification, precise amounts of internal standards were added and mixed homogenously with DMSO-d_6 solution, which are hexafluorobenzene (C_6F_6) for ^{19}F NMR (LiFSI) and acetonitrile (CH_3CN) for ^1H NMR (DME and HFC). Taking LiFSI consumption in SRCE as an example, the ^{19}F spectrum was processed with Mestre Nova software. As shown in **Figure R6d**, the peak of hexafluorobenzene (δ = -162.6 ppm) was integrated and normalized to 1.0000 ($I_{C_6F_6}$), whereas the peak of LiFSI (δ = -53.19 ppm) was

then integrated with a relative integral value of 0.1876 (I_{LiFSI}). Considering that one hexafluorobenzene molecule contains six equivalent fluorine atoms and one LiFSI molecule contains two equivalent fluorine atoms, the quantitative relationship is:

$$\frac{I_{LiFSI}}{I_{C_6F_6}} = \frac{2 \cdot n_{LiFSI}}{6 \cdot n_{C_6F_6}}$$

Thus, the remaining amount of LiFSI can be calculated as:

$$n_{LiFSI} = \frac{I_{LiFSI}}{I_{C_6F_6}} \times 3 \times n_{C_6F_6}$$

With the known mass of hexafluorobenzene added (11.6 mg, corresponding to 6.2347×10^{-5} mol), the remaining LiFSI was determined. The initial LiFSI content in the assembled cell was calculated based on the exact mass of electrolyte added (26.9 mg SRCE, containing 4.71×10^{-5} mol LiFSI). The LiFSI retention percentage was then obtained as (**Figure R6e**):

$$Retention(\%) = (\frac{n_{LiFSI,remaining}}{n_{LiFSI,initial}}) \times 100\%$$

For ^{1}H NMR quantification of DME and HFC, acetonitrile (CH_3CN) was used as an internal standard following a similar calculation principle.

For energy density calculation, the reported energy density of the 6 Ah pouch cell is calculated based on the total mass of the entire pouch cell. This follows the industry standard for practical device-level energy density reporting. The key parameters are summarized in **Table R1**.

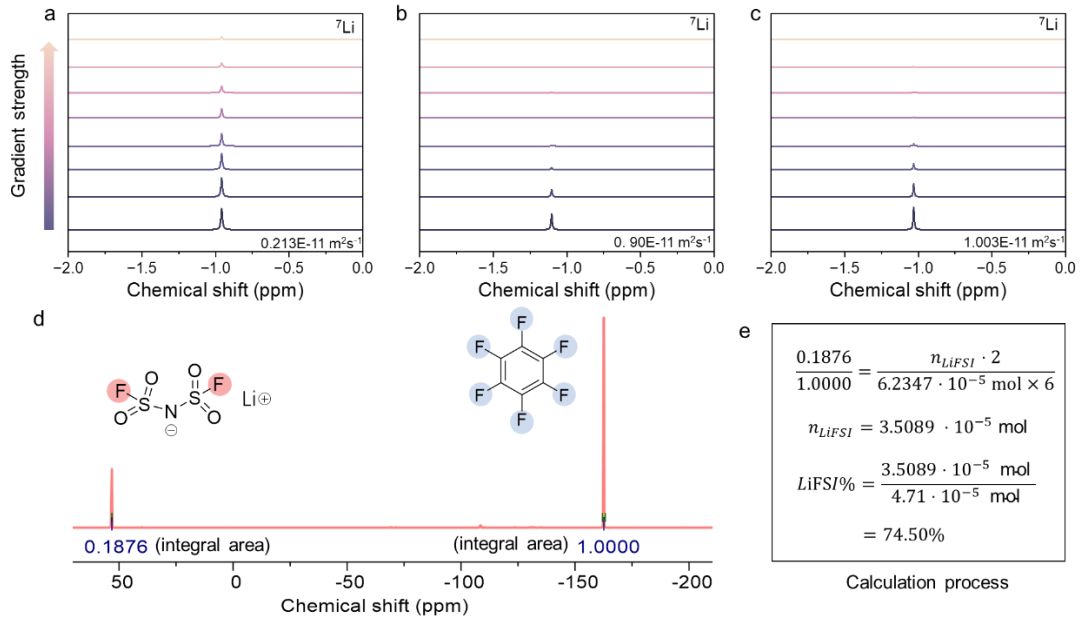

Figure R6. Pulsed field gradient nuclear magnetic resonance (PFG-NMR) spectra of ^{7}Li spectra

for (a) HCE, (b) LHCE, and (c) SRCE. (d) Quantitative ^{19}F NMR spectrum of the electrolyte achieved from the SRCE-based cell after 200 cycles, with peak integration performed using Mestre Nova software (hexafluorobenzene as internal standard). (e) Detailed calculation parameters and values for determining the residual amount of LiFSI in the SRCE electrolyte after cycling.

Table R1. Specific parameters of the 6 Ah-level Li metal pouch cell.

Component	Parameter	Value
Positive electrode $LiNi_{0.95}Co_{0.3}Mn_{0.2}O_2$	Active material loading	97 %
	Press density	3.2 g cm^3
	Dimensions	54*122 mm^2
	Mass Loading (Single-sided)	25 mg cm^2
	Collector	Al 12 μm
Negative electrode Li metal	Thickness	100 μm
	Dimensions	56*125 mm^2
Electrolyte	Weight	5.6 g
Separator	Celgard	20 μm
Total mass	-	44.372 g
Charge energy	at 0.1C	25.454 Wh
Discharge energy	at 0.1C	23.060 Wh
Energy density	at 0.1C	519 Wh kg^{-1}

We thank the reviewer again for pointing out these deficiencies and we have added the above-mentioned information in the **revised Manuscript** and **Supplementary information**.

Reviewer #2:

This paper reports a new electrolyte, sterically regulated high-concentration electrolytes (SHCE), by employing nonflammable fluorinated alkane HFC molecules for Li metal batteries. Owing to their low polarizability, the HFC molecules are suggested to alter the solvation structure, forming the smaller nanoclusters of ion pairs, which is supported by NMR and WAXS characterization. The SHCE electrolyte then shows enhanced cycling performance, which is attributed to improved interfacial stability at both the Li metal anode and NCM cathode, in addition to its excellent safety performance. Overall, the paper is well-written, and the proposed electrolyte demonstrates superior performance based on robust characterization and evaluation. I recommend publication of this work in Nature Communications, but there are several points to be addressed before publication.

Response: We thank the reviewer for the encouraging comments and insightful suggestions. We have incorporated additional experiments and analyses in response to the reviewer's suggestions. Our point-to-point replies to the comments are detailed as follows.

1. Regarding the interfacial stability on the Li metal anode side, the authors show the highest C-F signal in the SHCE electrolyte, which should be attributed to the decomposition of HFC diluent molecules. However, in the earlier section, the author proposed that the HFC interacts weakly with both cations and anions, which would minimize the contribution of HFC to SEI formation. The author should clarify this apparent inconsistency and revise the discussion accordingly. Or it seems that the peak assigned to C-F in the SRCE electrolyte shows a noticeable shift in peak position compared to the others. The author should consider other possible candidates for SEI components in the SRCE electrolyte, or provide a clear explanation for the origin of peak shift.

Response: We sincerely appreciate the reviewer for pointing out this error. Indeed, the peak at 687.6 eV in the F *1s* spectrum should be assigned to S-F rather than C-F. We have re-conducted and deconvoluted the XPS characterizations on the cycled Li metal surfaces across all three electrolytes.

As shown in **Figure R7a**, the peak observed at approximately 687.5 eV in the F *1s* spectrum is attributed to S-F bonds, which originate from incompletely reduced intermediates

of FSI^- anions (e.g., $-SO_2F$ derivatives)[1, 3]. Notably, the more direct evidence is that HCE electrolyte consists solely of LiFSI and DME, with no fluorinated diluents (i.e., no C-F bonds) in its formulation. Therefore, this peak could be unambiguously assigned to S-F species arising from FSI^- decomposition, rather than to C-F bonds originating from diluent decomposition.

To conclusively investigate the diluent decomposition, we present the corresponding high-resolution C *1s* spectra (**Figure R7b**). The decomposition of the diluent would inevitably cause the appearance of C-F signals around 292-294 eV in the C *1s* spectrum[4, 5]. However, the newly acquired C *1s* spectra show no detectable C-F signals in the LHCE and SRCE-derived SEI. These results clearly demonstrate that the fluorinated diluents remain chemically inert at the interface during Li plating/stripping. Furthermore, the strong cation-anion coordination in SRCE enables the preferential anion decomposition with an inorganic-rich interface. Therefore, the nanocluster design of SRCE leads to the formation of a highly rigid, inorganic-rich SEI matrix dominated by LiF. In contrast, for HCE and LHCE, the incompletely decomposed F-S species are embedded within a thick, polymer-like, organic-rich matrix, as evidenced by the strong C-O/C=O peaks. Moreover, the quantitative NMR analysis further confirms the stability of the fluorinated diluents during long-term cycling. To reduce the evaporation of the diluent during sample preparation, we completely redesigned the quantitative extraction protocol (see detailed information in our response to your **Comment 4**). The quantitative NMR data reveal a remarkable 97.3% retention of the HFC diluent in SRCE after 200 cycles. Since HFC is virtually unconsumed on a macroscopic scale, it mathematically cannot contribute substantially to the formation of the SEI layers. Therefore, the XPS and quantitative NMR data collectively demonstrate that the F signals at ~687.5 eV are attributed to S-F bonds and that the fluorinated diluents are chemically stable during cycling, supporting our original statements.

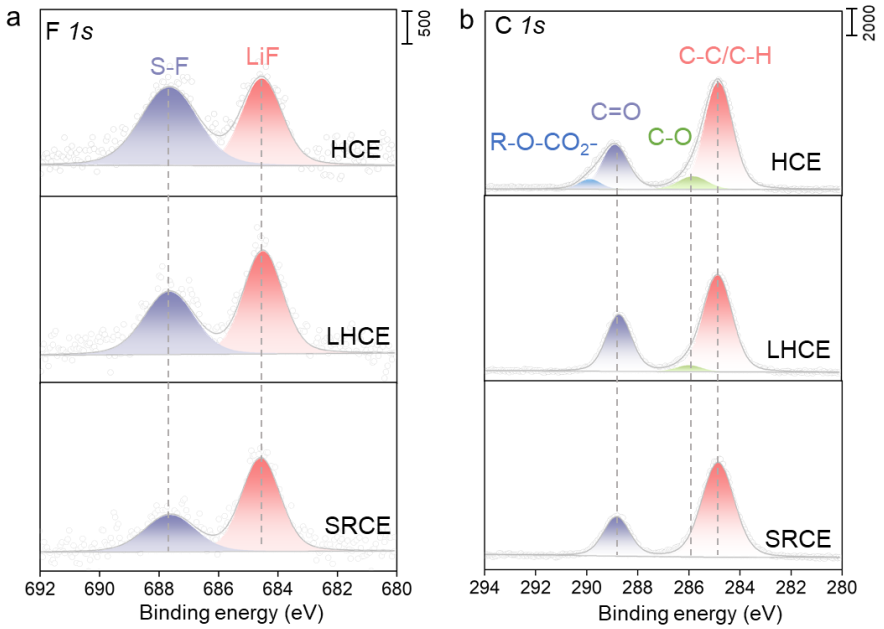

Figure R7. The XPS profiles of (a) F *1s* and (b) C *1s* spectra of the LMA's SEI chemistry cycled in Li||Cu cells with three electrolytes (0.5 mA cm^{-2}, 3 mAh cm^{-2}).

Revised Manuscript:

"*The high-resolution F 1s spectra demonstrate a substantially higher proportion of Li-F signal in SRCE compared to the more prominent S-F signal observed in both LHCE and HCE, arising from incomplete decomposition of FSI^- anions (**Figure 3f**). Corresponding C 1s spectra show more intense carbon-related signals in HCE and LHCE, indicating a higher content of organic species in their SEIs (**Supplementary Figure 11**). Unfortunately, these organic composites are likely to originate from solvent decomposition, which subsequently consumes electrolyte, impedes Li^+ transportation, and accelerates lithium dendrite growth.*" (**Page 8**, **Line 204**)

2. Moreover, it is surprising that the introduction of HFC leads to highly dense and planar Li microstructure. Not only LiF contents, the author should also include the analysis of other critical SEI components, such as Li_2O, which might have an impact on such Li morphology, considering that LiF is well known to be mechanically robust.

Response: We thank the reviewer for the insightful suggestion. To precisely analyze the composition of the SRCE-derived SEI, we have further employed XPS depth profiling combined with 3D TOF-SIMS to precisely map the chemical identity and spatial distribution of Li_2O within the SEI.

As shown in **Figure R8a-c**, we monitored the compositional evolution of the SRCE-derived SEI across increasing sputtering depths. The organic species, e.g., C=O and C-C/C-H, are prominent at the SEI surface. Upon Ar sputtering, the organic carbon signals decay markedly, indicating suppression of solvent decomposition. Correspondingly, the O *1s* spectra reveal a massive and dominant emergence of inorganic Li_2O, which intimately coexists with the highly enriched LiF. These results provide unambiguous evidence that the preferential decomposition of FSI^- anion enables the formation of an ideal "dual inorganic" inner SEI, composed of both rigid, insulating LiF and highly conductive Li_2O. Therefore, the mechanical robust and high Li^+ conductivity of the as-formed inorganic-rich SEI layer could suppress the interfacial parasitic reactions, including dendrite growth and electrolyte decomposition, and lead to the plating of the highly dense and planar Li morphology.

Furthermore, we investigated the 3D TOF-SIMS to systematically compare spatial distribution of Li_2O across three electrolytes. The sputtering depth profile shows that the SRCE-derived SEI exhibits a significantly higher, more continuous, and stable intensity of Li_2O fragments throughout SEI, consistent with the XPS results (**Figure R8d**). In contrast, the LHCE shows an overall depleted Li_2O signal. Notably, the HCE shows a severely depressed Li_2O signal at SEI surface, while only at greater depths does the signal increase. This indicates a highly heterogeneous SEI covered by a thick layer of sluggish organic byproducts. The 3D reconstructed maps further visually display that the Li_2O network in the SRCE-derived SEI is exceptionally dense, uniform, and pervasive, compared with the sparse, non-uniform architectures observed in LHCE and HCE. Consequently, the XPS depth profiling and TOF-SIMS results collectively demonstrate the addition of HFC diluent enables weak diluent-ion pairs interactions to promote isolated nanocluster formation, thereby accelerating the anion decomposition to form a thin and inorganic-rich SEI layer.

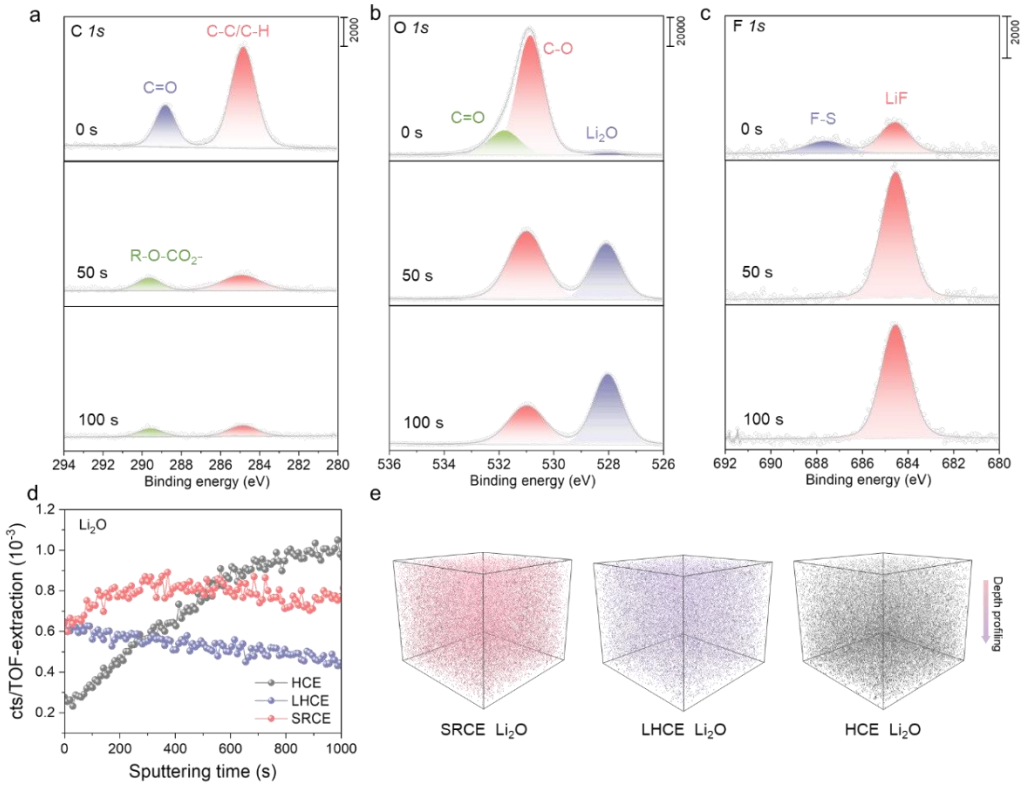

Figure R8. XPS results with depth profiles of (a) C *1s* , (b) O *1s*, and (c) F *1s* spectra of the SEI formed on the cycled LMA interface after cycled in Li||Cu cell with SRCE electrolyte (0.5 mA cm^{-2}, 3 mAh cm^{-2}). (d) Sputtering depth profiles of Li_2O fragments distribution in the SEI by TOF-SIMS. (e) Three-dimensional TOF-SIMS maps showing the variation of Li_2O signal intensity as a function of depth for the SEI on cycled Li anodes from three electrolytes.

Revised Manuscript:

"*The high-resolution F 1s spectra demonstrate a substantially stronger Li-F signal in SRCE compared to the more prominent S-F signal observed in both LHCE and HCE, arising from incomplete decomposition of FSI⁻ anions (**Figure 3f**). Corresponding C 1s spectra show more intense carbon-related signals in HCE and LHCE, indicating a higher content of organic species in their SEIs (**Supplementary Figure 11**). Unfortunately, these organic composites are likely to originate from solvent decomposition, which subsequently consumes electrolyte, impedes Li^+ transportation, and accelerates lithium dendrite growth. Moreover, the XPS depth profiling reveals an inorganic-rich SEI formed in SRCE, featuring a massive and dominant presence of LiF that intimately coexists with highly enriched Li_2O (**Supplementary Figure 12**).*"

(**Page 8**, **Line 204**).

"The 3D reconstruction of TOF-SIMS images confirms that the SEI formed in SRCE exhibits a homogeneous and abundant distribution of LiF with minimal organic carbon, consistent with the XPS results." (**Page 9**, **Line 217**)

3. For SEI structure analysis, it is suggested to perform cryo-TEM analysis to show thin and robust CEI as shown in the schematic of Figure 1.

Response: We thank the reviewer for this highly constructive suggestion. To provide direct, atomic-scale visual evidence of the "thin and robust" cathode electrolyte interface (CEI), we have further conducted the Cryogenic Transmission Electron Microscopy (Cryo-TEM) and the Spherical Aberration-Corrected Transmission Electron Microscopy (AC-TEM), following your guidance.

To ensure a sufficiently mature CEI layer for accurate compositional analysis while also demonstrating long-term structural stability, we characterized a cathode harvested after 200 cycles in SRCE, rather than the 50 cycles reported in the original manuscript. Cryo-TEM clearly captured a thin (~10 nm), homogeneous, and conformal CEI formed on the NCM811 surface (**Figure R9a**). Unfortunately, owing to the resolution limits of our instrument (FEI Talos F200C) under the low electron-dose conditions required for cryo-imaging, we were not able to resolve atomic-scale crystalline lattices and therefore could not directly confirm the robust inorganic nature of the interphase.

Unlike the fragile solid electrolyte interphase (SEI) on the highly reactive Li metal anode, the CEI is relatively stable against the electron beam. Therefore, we subsequently turned to AC-TEM on the same 200-cycle cathode to overcome the technical barrier (**Figure R9b**). The AC-TEM results represent a clear advance in our structural analysis and strongly support our hypothesis in **Figure 1**. Even after 200 cycles, the CEI remains compact and smooth, with no sign of uncontrolled amorphous thickening. The high-resolution image further revealed a dense array of inorganic nanocrystals embedded in the CEI matrix, dominated by LiF and Li_2O. This unique architecture not only suppresses electrolyte decomposition and facilitates Li^+ migration but also enhances mechanical strength, thereby suppressing particle cracking and transition-metal dissolution (**Figure R9c-e**). Therefore, the CEI formed in the SRCE could efficiently protect the cathode materials and enable a long-term cycling performance.

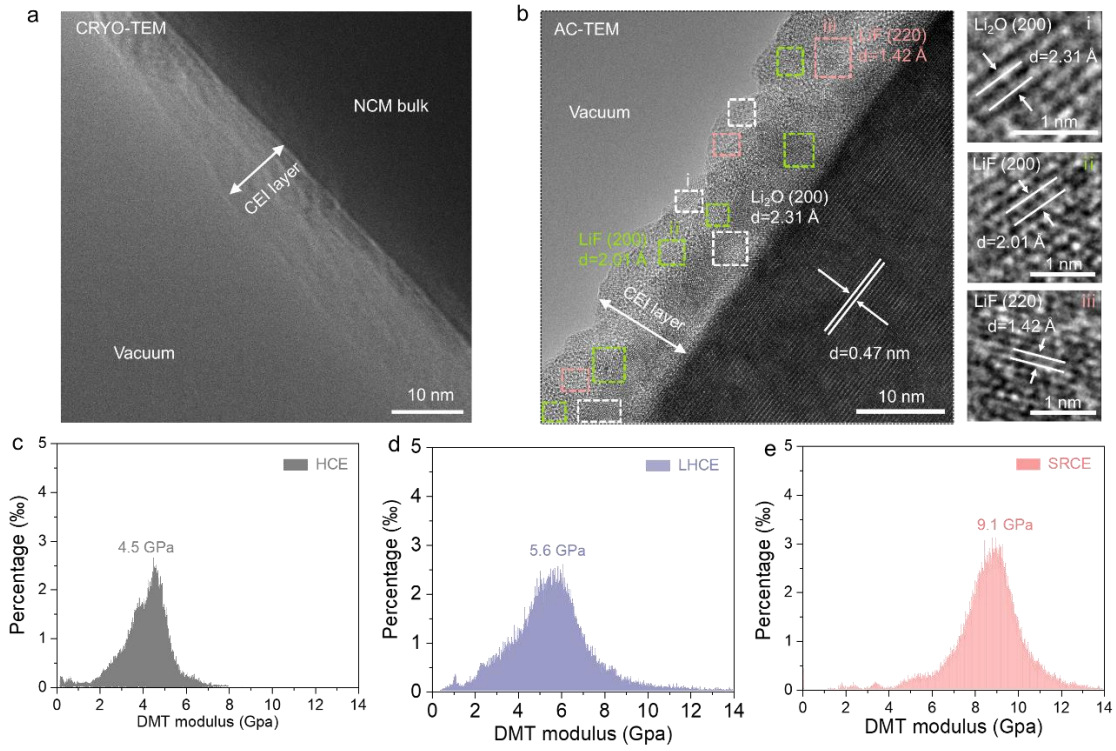

Figure R9. (a) Cryo-TEM image of the cathode electrolyte interphase (CEI) formed on an NCM811 cathode after 200 cycles in SRCE electrolyte. (b) AC-TEM image (left) and the corresponding high-resolution image (right) of the as-formed CEI. (c) Derjaguin-Muller-Toporov (DMT) modulus maps acquired by Atomic Force Microscopy in Quantitative Nanomechanical Mapping (AFM-QNM) mode for cathodes cycled in (c) HCE, (d) LHCE, and (e) SRCE.

Revised Manuscript:

"*The CEI protection layer comprises a dense array of embedded inorganic nanocrystals, dominated by LiF and Li_2O (**Supplementary Figure 23**). This structure could inhibit electron transfer and nucleophilic attack by electrolytes, thereby suppressing oxygen loss and transition metal (TM) dissolution, which are the culprits behind Li/Ni cation mixing and rock-salt phase formation.*" (**Page 13**, **Line 303**)

4. In Figure 5i, the authors quantitatively analyzed the remaining amounts of diluents, LiFSI and DME after 200 cycles, but the results appear to be overestimated. If it is true, it would be questionable how those cells can work for prolonged cycles (Figure 4b) even with such large electrolyte loss. Previous work (https://doi.org/10.1038/s41565-025-01935-y) reported that

LiFSI consumption is the dominant source of electrolyte loss, whereas the amounts of DME and TTE remain relatively constant. Moreover, in both LHCE and SRCE, diluents are consumed more than DME despite their minimal participation in the solvation sheath and increased oxidation stability. The author should clearly describe the experimental procedure used for the NMR-based quantification and discuss the origin of the apparently large solvent consumption, particularly diluents.

Response: We are grateful to the reviewer for identifying this critical discrepancy and providing a helpful reference. Accordingly, we have redesigned the sample preparation protocol to minimize salt and solvent consumption during rinsing, thereby enabling more accurate NMR quantification.

The abnormal electrolyte consumption is attributed to physical evaporation and incomplete extraction rather than actual electrochemical degradation. As shown in **Figure R10a**, the original method employed a rinsing process: the cycled cells were disassembled in the glovebox and washed dropwise with DMSO-d_6. Unfortunately, because HFC (b.p. 83° C), DME (b.p. 83° C), and TTE (b.p. 92° C) are highly volatile, this handling inevitably led to massive and immediate solvent and diluent losses by evaporation. Moreover, the residual, viscous LiFSI salts are trapped deeply within the porous separator and NCM811 cathodes, which could not be fully extracted by brief surface washing. Collectively, cumulative procedural flaws severely underestimated the remaining electrolyte, giving the false impression of "extreme consumption" in our previous statement.

To minimize electrolyte consumption caused by improper operation, we developed an improved extraction protocol, as illustrated in **Figure R10b**. After disassembling the cycled cells, all internal components (electrodes, separators, spacers, spring, and casing) were immediately submerged in a centrifuge tube pre-filled with 2mL DMSO-d_6. The tube was then sealed without delay, vigorously vortexed, and left to rest for 12 hours to extract the remaining electrolyte. This evaporation-free protocol ensures maximum dissolution of all residual electrolyte species directly from the cell components. To guarantee statistical reliability, four independent parallel cells (n=4) were tested for each condition.

The newly acquired quantitative NMR data correct the previous overestimations. As shown in the cycle-dependent evolution for the SRCE, LiFSI consumption is indeed the

dominant source of electrolyte loss (**Figure R10c**). This phenomenon is driven by its continuous decomposition to form and repair the inorganic-rich SEI/CEI, consistent with the previous reference[1, 5]. DME shows a moderate decline over cycling, whereas the diluent remains highly conserved throughout all cycles. Admittedly, it is worth noting that the absolute consumption percentages differ from literature values due to unavoidable variations in extraction protocols, cell configurations, and initial electrolyte-to-capacity (E/C) ratios. However, the fundamental hierarchy and relative trends of component depletion remain fully consistent with their findings. After 200 cycles, the measured retention of the HFC diluent in SRCE is 97.3%, compared to 94.7% for TTE in LHCE (**Figure R10d**). These results explicitly confirm that uncoordinated diluents are chemically inert and do not contribute significantly to SEI formation, corroborating our XPS analysis in response to your **Comment 1**. Furthermore, these comparative data robustly reinforce the advantage of the SRCE design in preserving the liquid electrolyte inventory. After 200 cycles, SRCE significantly mitigates electrolyte exhaustion, retaining 74.5% of LiFSI and 85.7% of DME. This performance far exceeds that of LHCE (58.8% LiFSI, 78.8% DME) and HCE (severely depleted to 46.1% LiFSI and 62.1% DME). The improvement arises because the HFC diluent, with weak diluent-ion interactions, facilitates the formation of isolated nanoclusters with strong Li^+-FSI^- interactions, thereby accelerating anion decomposition and producing a thin, robust, inorganic-rich SEI layer that suppresses electrolyte decomposition. Therefore, this effective preservation of the electrolyte inventory underpins the prolonged cycling lifespan of our cells.

In summary, correcting this methodological flaw has greatly enhanced the integrity of our study. The revised results demonstrate that the HFC diluent remains virtually unconsumed. Moreover, the formation of isolated solvation nanoclusters promotes Li^+ transport kinetics to suppress dendrite formation, while forming a robust, inorganic-rich SEI/CEI that effectively suppresses parasitic reactions and electrolyte decomposition. The combination of diluent inertness, favorable interphase chemistry, fast Li^+ transport kinetics, and sustained electrolyte retention forms the true origin of the prolonged cycling performance.

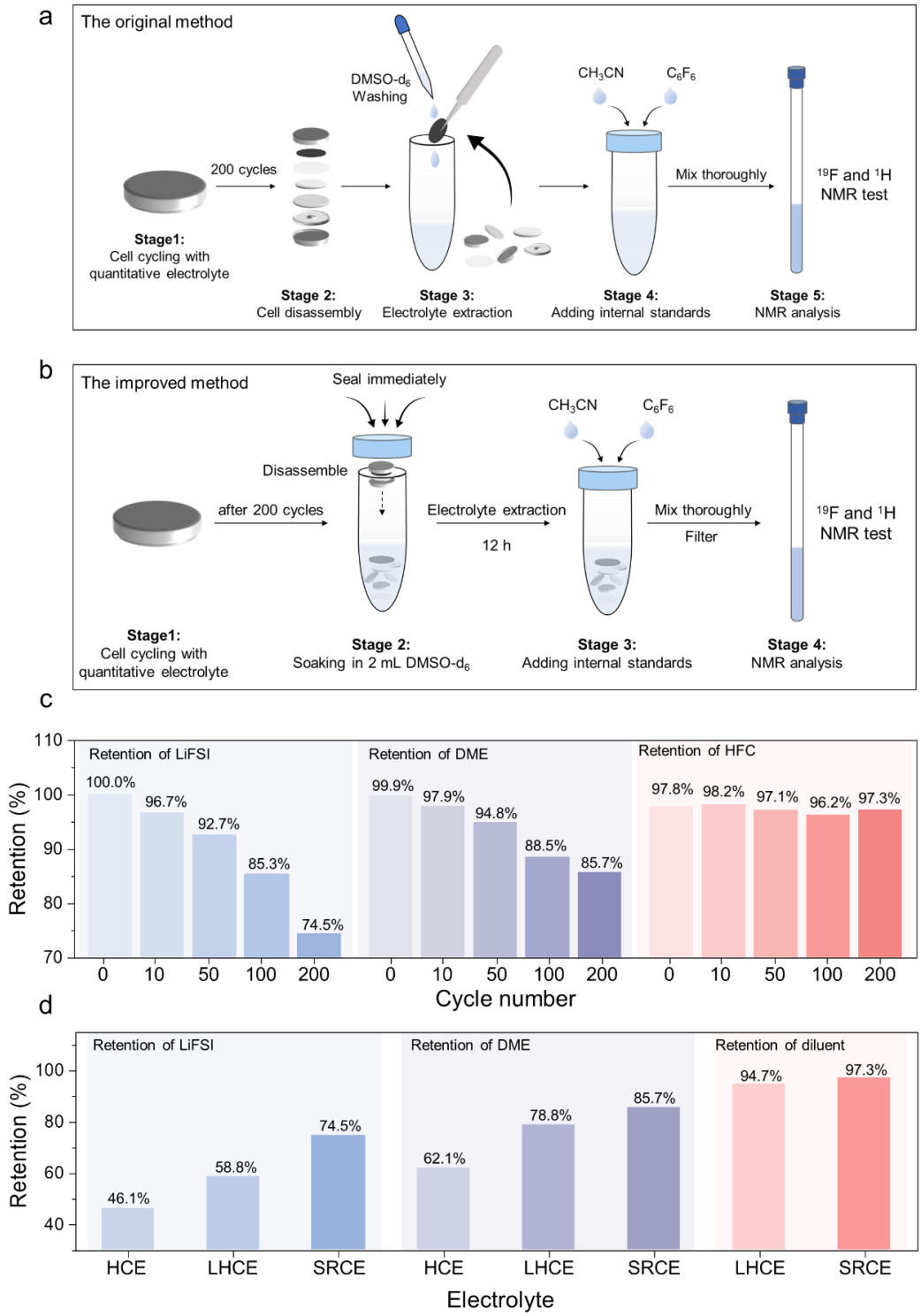

Figure R10. Schematics of (a) the original extraction method and (b) the modified method. (c) Cycle-dependent retention of LiFSI, DME, and HFC over 200 cycles for 50 μm Li|| 2.5mAh cm^{-2} NMC811 with SRCE electrolyte. (d) Quantitative comparison of LiFSI, DME, and diluent retention across three electrolytes after 200 cycles. Data are averages from 4 independent samples.

Revised Manuscript:

"*After 200 cycles under lean electrolyte conditions, HCE and LHCE consume 53.9% and 41.2% of LiFSI salt, respectively (**Figure 5i** and **Supplementary Figure 28-31**). Remarkably, SRCE suppresses salt decomposition to 25.5%, together with minimized diluent and solvent consumption, confirming that effective CEI sufficiently mitigates failure modes associated with electrolyte exhaustion, thereby enhancing practical cycling performance*." (**Page 14**, **Line 333**)

"*Quantitative NMR spectroscopy was employed to analyse electrolyte evolution after 200 cycles (**Supplementary Figure 46** and **Supplementary Note 3**). 2.5 mAh cm^{-2} NCM811|| 50 μm Li full cells with precisely recorded electrolytes were disassembled in an argon-filled glovebox after cycling. All internal components were immediately submerged in a centrifuge tube pre-filled with 2 mL DMSO-d_6. The tube was then sealed without delay, vigorously vortexed, and left to rest for 12 hours. For internal referencing, precisely weighed amounts of acetonitrile and hexafluorobenzene were added for ^{1}H and ^{19}F analyses, respectively. The NMR spectra were acquired on a Bruker AVANCE NEO 400 MHz spectrometer and four independent parallel cells were tested for each condition to ensure statistical reliability.*" (**Page 21**, **Line 504**)

5. In page 6 line 150, HSP distance appears first without its full name.

Response: We sincerely thank the reviewer for catching this error. The abbreviation "HSP" has now been properly introduced with its full name, "Hansen Solubility Parameters", at its first appearance in the main text to ensure clarity for the readers. We have further checked the entire **Manuscript** to ensure that all abbreviations are defined on first use.

Revised Manuscript:

"*...based on Hansen Solubility Parameters (HSP), mutual solubility is governed by...*" (**Page 3**, **Line 72**)

Reviewer #3:

The manuscript by Du and coworkers presents a thorough characterization study of a novel localized high concentration electrolyte (LHCE), in which a diluent is added to a concentrated electrolyte to yield two nano-segregated phases, an ion-conducting salt phase and a diluent phase. In particular, the authors' work revolves around the concept that the diluent should distort the lithium solvation shell as weakly as possible. To this purpose, conventional diluents, typically fluorinated ethers, are replaced by a fluorinated cycloalkane which shows weaker interactions with the lithium solvation shell, as demonstrated by NMR and vibrational spectroscopy as well as Density Functional Theory calculations and Molecular Dynamics simulations. The battery cells utilizing this novel electrolyte show superior performance in extensive cell test. In my opinion, the manuscript could be of interest for Nature Communications if the central design concept would be scrutinized in more detail as detailed below. Otherwise, the study would rather reflect a thorough (and well-done) characterization study of a specific electrolyte formulation, which might be better suited for a more specialized journal. For a prestigeous journal such as Nature, more general takeaway messages and/or design principles that leave a broad impact in the field would be required.

Response: We sincerely thank the reviewer for recognizing the value of our work and for raising insightful suggestions. We agree that the key design concept was not presented with sufficient clarity in the original **Manuscript**, and some related terms were imprecise. To address this, we have performed additional experiments and explanations to substantially revise the relevant sections. Below, we first summarize our refined hypothesis and design principle, which we believe now more clearly articulate the unique advantage of our diluent and its broad implications for LHCE design.

Firstly, the diluent selection is guided by Hansen solubility parameters (HSP). The diluent should have an optimal HSP distance that minimizes interactions between the diluent and ion aggregates (including cations, anions, and solvents) while still ensuring miscibility in the high-concentration electrolyte (HCE). Secondly, we acknowledge that, like conventional diluents, the addition of HFC alters the Li^+ first solvation sheath by partially replacing DME with FSI^- anions. However, the weak diluent-solvent/anion interactions and the modestly increased anion coordination counteract each other. As a result, the electron density around Li^+ is preserved,

thereby the Li^+-FSI^- interaction is stronger than that in a typical LHCE due to the inductive effect, which promotes the formation of an inorganic-rich interphase. Moreover, the larger HSP distance of HFC disrupts the medium-range CIP aggregates network, breaking them into isolated nanoclusters. This configuration could facilitate Li^+ transport kinetics, leading to higher ionic conductivity, suppressed lithium dendrite formation, and improved rate capability. Finally, cross-swap experiments reveal that the bulk electrolyte governs ion transport and interfacial desolvation to enhance rate capability, whereas the interphase suppresses parasitic reactions and ensures interfacial stability to prolong cycle life. Together, these distinct yet complementary roles underpin the promising electrochemical performance of SRCE.

We have further incorporated additional experiments and detailed analyses in response to the reviewer's suggestions. Our point-to-point replies to the comments are detailed below.

1. In particular, the authors' key hypothesis is that the solvation shell is not perturbed in the novel SRCE as compared to the underlying high-concentration electrolyte (HCE), in contrast to an LHCE using the conventional TTE diluent. If this was true, the lithium-ion solvation shells in the HCE and the SRCE should be identical and lead to very similar electrolyte decomposition products at the electrode interface. However, experimentally, the authors find different compositions for all three electrolytes (HCE, LHCE, and SRCE). Here, I am wondering in how far this contradicts the authors' hypothesis.

Response: We sincerely thank the reviewer for this insightful comment regarding our hypothesis. We agree that the original phrasing "mitigate the perturbations of solvation structures" is imprecise, as adding a miscible diluent inevitably influences the Li^+ solvation structure. Our key hypothesis, supported by theoretical simulations and physical characterization, is that the diluent should minimally interact with cations, anions, and solvents. This approach mitigates the diluent's influence on the interaction between Li^+-FSI^- while dispersing its medium-range aggregate network into isolated nanoclusters.

We first acknowledge that the geometric composition of the Li^+ first solvation shell in SRCE is closer to that in LHCE than to that in HCE. This phenomenon is a general consequence of introducing low-polarity fluorinated diluents. To remain miscible with the HCE, the diluents should interact with DME via hydrogen bonding, competitively displacing solvent molecules

from the Li^+ solvation sheath and promoting anion ingress. This diluent-induced solvent-anion exchange is well-documented for LHCEs[6-8]. Accordingly, the coordination numbers (CNs) derived from MD simulations show Li^+-O(DME) values of 2.15, 1.70, and 1.77 for HCE, LHCE, and SRCE, respectively, with Li^+-O(FSI^-) values correspondingly increasing from 2.81 to 3.57 and 3.51 (**Figure R11a**, see **Comment 5** for detailed information). Although the influence of HFC is smaller than TTE for CNs, the expression "mitigate the perturbations of solvation structures" appears exaggerated. Therefore, we have corrected this imprecise expression in the revised **Manuscript**.

Although the coordination numbers of FSI^- increase similarly in LHCE and SRCE, the electronic environment perturbation of Li^+ imparted by the two diluents differs markedly. TTE forms stronger hydrogen bonds with FSI^- (total H-bond energy 90.8 kJ mol^{-1}, **Figure R11b**, see **Comments 4** for detailed information), withdrawing electron density from the anion and weakening its electron-donating capability toward Li^+. Therefore, the ^{19}F signal of FSI^- in LHCE shifts upfield by 0.75 ppm, while the ^7Li signal exhibits a downfield shift despite the increased anion coordination (**Figure R11c** and **e**). In contrast, the HFC with non-heteroatom coordination sites and a large steric effect possesses low polarizability and a low dielectric constant. As shown in **Figure R11b**, the HFC diluents interact weakly with both FSI^- (59.5 kJ mol^{-1}) and DME (34.9 kJ mol^{-1} vs 45.4 kJ mol^{-1} for TTE-DME). Reflecting this weak-interaction landscape, the ^{19}F shift of FSI^- and the ^{17}O shift of DME in SRCE are attenuated to -0.56 ppm and -0.94 ppm, respectively, both smaller than those induced by TTE. More importantly, due to the attenuated competing diluent-anion interactions, the modestly reduced electron-donating ability and the slightly increased anion coordination counterbalance each other. As a result, the ^7Li shift of SRCE differs from that of HCE by only -0.007 ppm. The meaningful invariant of a "non-perturbed solvation" is therefore the chemical environment of Li^+ and the interaction between Li^+ and FSI^-, not the geometric composition of the first solvation shell. According to previous references, the stronger cation-anion interaction in SRCE could promote the formation of inorganic-rich interphases with favorable chemical, mechanical, and thermal stability, without degrading the Li^+ transport kinetics as observed in HCE[8, 9].

Beyond the Li^+-FSI^- interactions in the first solvation shell, the second key advantage of the HFC diluent concerns the mesoscale organization of ion pairs, governed by diluent-CIP

miscibility via Hansen solubility parameters (HSP). The cyclic, saturated, weakly polar HFC combines low dispersion, polar, and hydrogen-bonding contributions, yielding an HSP distance to the CIP phase substantially larger than that of TTE (See **Comments 3** for detailed information). This thermodynamic incompatibility, reinforced by the steric demand of the cyclopentane skeleton, disassembles the medium-range aggregate network of CIPs and isolates individual CIPs into smaller, randomly distributed nanoclusters. Therefore, the WAXS results demonstrate that the bimodal HCE features at 0.94 $Å^{-1}$ (inter-cluster correlation) and 1.54 $Å^{-1}$ (direct cation-anion contact) collapse into a single broad peak centered at 1.21 $Å^{-1}$ in SRCE (**Figure R11f**). In contrast, LHCE retains both peaks at reduced intensity, reflecting partial but incomplete dissociation of medium-range aggregation, consistent with the residual participation of TTE in anion solvation. Consequently, the isolated CIPs promote Li^+ transport kinetics, resulting in higher ionic conductivity, suppressed Li dendrite formation, and improved rate performance.

As for the different compositions of the SEI formed in the three electrolytes, although the Li^+-FSI^- interaction is similar in SRCE and HCE, the distinct solvation structures, aggregate clusters, and transport kinetics lead to different reaction environments, ultimately producing different SEI compositions across the three systems.

In conclusion, what distinguishes SRCE from a conventional LHCE is therefore not the geometry of the Li^+ first solvation shell, but the simultaneous preservation of the strong Li^+-FSI^- interaction found in HCE and the dispersion of its medium-range aggregate network into isolated nanoclusters. This unique combination promotes the formation of an inorganic-rich SEI and enhances transport kinetics, resulting in the observed performance improvement at the pouch cell level.

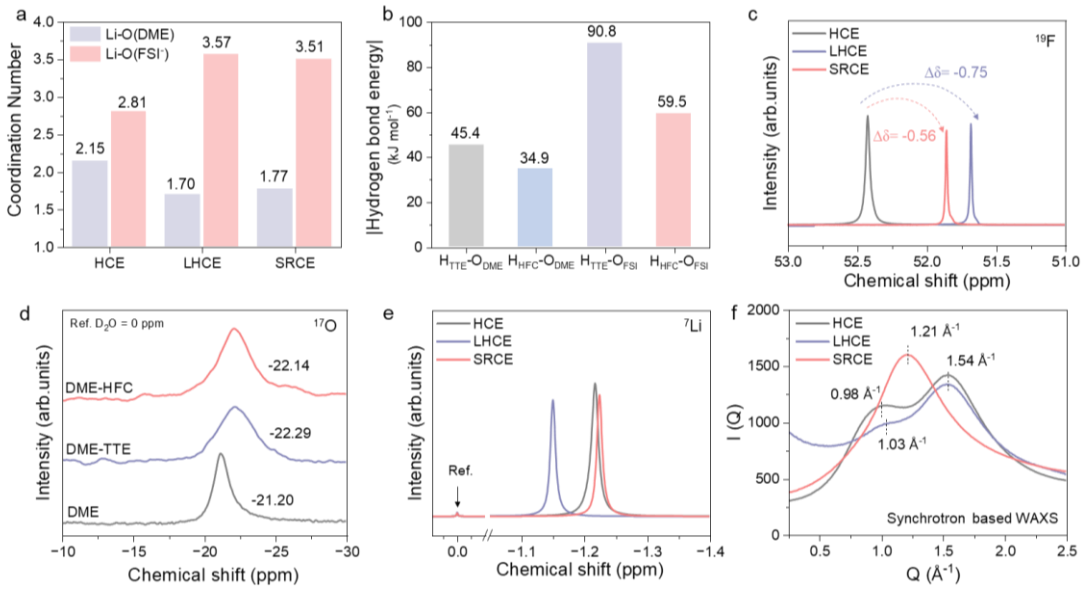

Figure R11. (a) Coordination number (CN) of Li^+ within the first solvation shell (r=3 Å) extracted from molecular dynamics (MD) simulations. (b) Comparison of the total absolute hydrogen-bond binding energies for the respective diluent-solvent and diluent-anion interactions. (c) ^{19}F NMR spectra of FSI^- in three electrolytes (external reference: 1M $Zn(OTF)_2$ in D_2O at -78.84 ppm). (d) ^{17}O NMR spectra of DME solvent, DME-TTE mixture, and DME-HFC mixture (external reference: D_2O at 0 ppm). (e) ^{7}Li NMR spectra of three electrolytes (external reference: 1M LiCl in D_2O at 0 ppm). (f) Synchrotron wide-angle X-ray scattering profiles of three electrolytes.

Revised Manuscript:

"*More importantly, these diluents interact relatively strongly with both anions and solvents. The diluent-anion interaction disrupts Li^+-anion coordination and weakens the Li^+ inductive effect, thereby diminishing the inorganic content in both interfacial layers*[31]. *Furthermore, although the anchoring effect arising from the diluent-solvent interaction reduces solvent decomposition, it fails to sufficiently break down the bulky aggregates, considerably impeding Li^+ transport kinetics*[32]." (**Page 3**, **Line 62**)

"Rational design of non-flammable diluents, through modulation of molecular structure, spatial configuration, and functional groups, offers a promising route to enhance immiscibility, thereby minimizing diluent interference with ionic aggregates and promoting the formation of isolated and stable nanoclusters in LHCEs." (**Page 3**, **Line 73**)

"*Herein, we propose a novel diluent strategy to mitigate diluent interactions with Li^+ cations,*

*solvents, anions, and their ionic aggregates. By employing nonflammable cyclic fluorinated alkane (1,1,2,2,3,3,4-Heptafluorocyclopentane, HFC) molecules with optimal intermolecular force, i.e., dispersion (δD), polar (δP), and hydrogen bonding (δH), between the diluent and ion pairs. Therefore, the designed diluent could be miscible in HCE and further promote the formation of isolated ionic aggregate nanoclusters (**Figure 1** and **Supplementary Table 1-2**).*" (**Page 3**, **Line 81**)

"*Consistent with previous literature, MD simulations demonstrate that the diluents interact with DME to competitively displace solvent molecules from the Li^+ solvation sheath and promote anion ingress, whereas the influence of HFC is smaller than that of TTE (**Supplementary Figure 5** and **Table 4**).*" (**Page 5**, **Line 129**)

"*This phenomenon may stem from attenuated competing diluent-anion interactions, in which the modestly reduced electron-donating ability and the slightly increased anion coordination counterbalance each other.*" (**Page 5**, **Line 136**)

2. Of course, I am aware that the transport is improved in the SRCE as compared to the HCE, which likely also affects the interface kinetics. Therefore, it is not entirely clear in how far the observed improved performance of the battery cells arises from the improved transport alone (which would be the case for a standard LHCE as well), the modified SEI/CEI composition, or a combination of both. For example, the transference number of the SRCE is larger than in the LHCE, which could improve cell performance independently from the modified SEI/CEI composition. Would it be possible to disentangle these effects? I believe that the manuscript would benefit if these aspects were discussed in more detail. This would also strengthen statements related to rational electrolyte design such as "Herein, we propose a novel diluent strategy to mitigate the perturbations of solvation structures, including Li^+ cations, solvents, and anions."

Response: We thank the reviewer for the thoughtful suggestion on distinguishing the effect of SEI/CEI and transport kinetics. The improvement is attributed to the combined effects of two factors. To disentangle the contribution of bulk transport and interphase chemistry to electrochemical performance, we designed a new cross-swap experiment in which the SEI/CEI and electrolyte are independently varied.

After two formation cycles, the electrodes carrying the formation-derived CEI/SEI (denoted as X-interphase) were transferred into a fresh cell filled with a same/different electrolyte (denoted as Y-electrolyte). This protocol could isolate the contributions of electrolyte bulk transport and LiF/Li_2O-rich interphase. As shown in **Figure R12a**, pairing an HCE-interphase with an SRCE-electrolyte could recover most of the SRCE's rate capability, while pairing an SRCE-interphase with an HCE electrolyte could preserve part of the rate performance. This phenomenon demonstrates that the high-t^+, high bulk-transport properties of the SRCE electrolyte contribute more to the enhanced rate capability (**Figure R12b**).

Moreover, the interphase contribution is independently confirmed under near-equilibrium conditions. As shown in **Figure R12c**, the 4.3 V floating leakage current after 20 cycles drops from 8 μA in HCE to 4 μA and 1 μA in LHCE and SRCE, respectively. Since the three electrolytes share comparable intrinsic oxidative onsets above the operating window, this reflects CEI passivation rather than bulk oxidation. The 24 h open-circuit voltage decay at full charge yields the same ranking, with ΔV values of 0.104 V, 0.098 V, and 0.046 V for HCE, SRCE, and LHCE, respectively, indicating suppressed parasitic reactions during high-voltage rest (**Figure R12d**). These results demonstrate that an inorganic-rich CEI/SEI effectively mitigates parasitic reactions and extends cycle life.

To investigate interphase evolution over prolonged cycling, we performed a long-term cross-swap experiment (**Figure R12e**). As cycling proceeds, the four cell configurations exhibit distinct trajectories. The HCE (interphase)-HCE (electrolyte) cell shows a slightly lower initial capacity due to sluggish Li^+ transport kinetics. The cell decayed within 200 cycles, underscoring that poor interphase chemistry, together with slow bulk transport, could not sustain long-term cycling at a moderately high rate of 1C. Furthermore, comparing SRCE (interphase)-HCE (electrolyte) with SRCE (interphase)-SRCE (electrolyte) reveals that an initially inorganic-rich interphase alone could not fully determine long-term performance. Instead, its evolution in subsequent cycles is strongly modulated by the solvation structure and kinetic properties of the surrounding bulk electrolyte. Conversely, a comparison between HCE (interphase)-SRCE (electrolyte) and SRCE (interphase)-SRCE (electrolyte) expounds that even when the bulk electrolyte is identical in later stages and an inorganic-rich interphase could gradually form during subsequent cycling, the nature of the initial interphase still exerts a non-

negligible influence on long-term cycling behavior.

Taken together, these results demonstrate that sustained long-term stability requires simultaneous contributions from both the bulk electrolyte and the interphase. The bulk electrolyte governs ion transport kinetics and the solvation environment, while the interphase dictates parasitic reaction suppression and interfacial stability. Neither factor alone is sufficient, where their functionally distinct yet mutually reinforcing roles collectively underpin the enhanced cycling performance of SRCE.

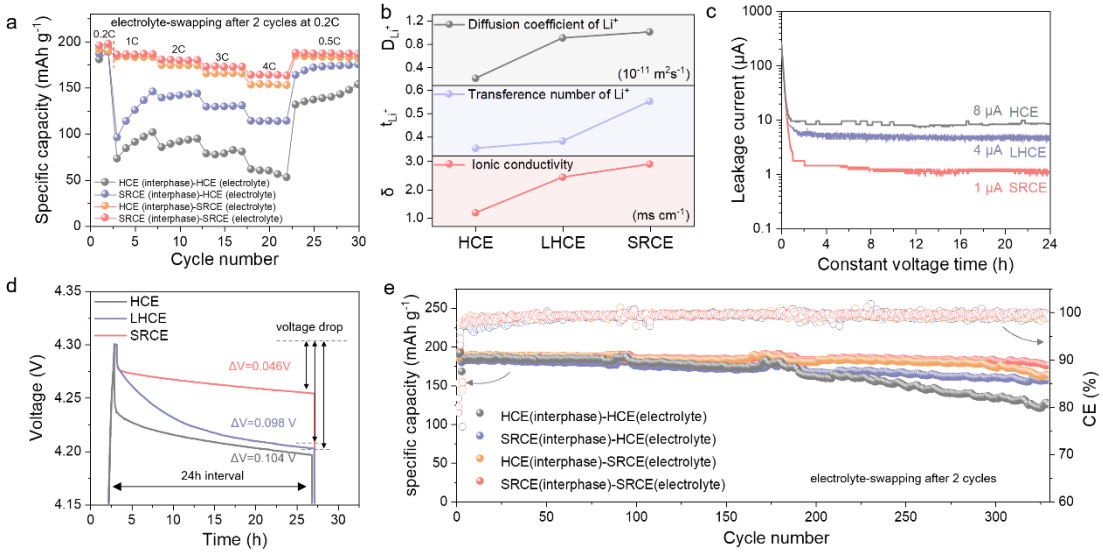

Figure R12. (a) Rate performance of 2 mAh cm^{-2} NCM811|| 50 μm Li cells in cross-swap configurations, where X (interphase)-Y (electrolyte) denotes electrodes pre-cycled in electrolyte X and transferred into fresh electrolyte Y after two formation cycles. (b) Li^+ transport properties in three electrolytes: Li^+ diffusion coefficient (D), Li^+ transference number (t_+), and ionic conductivity (δ). (c) Leakage current during 4.3 V constant-voltage floating performed test of 2.5 mAh cm^{-2} NMC811||50 μm Li full cells after 20 cycles. (d) Open-circuit voltage decay over 24 h at the fully charged state. (e) Long-term cycling performance of the cross-swap cells. Note: To exclude any artifacts arising from the cell disassembly procedure, all cells were subjected to an identical disassembly and reassembly protocol, including those for which the bulk electrolyte was kept unchanged before and after the swap.

Revised Manuscript:

"*Moreover, cross-swap experiments were conducted to disentangle the contributions of bulk transport and interphase chemistry to electrochemical performance (see **Methods** for detailed*

*information). As shown in the **Supplementary Figure 32**, the bulk electrolyte enhances rate capability by governing ion transport and interfacial desolvation, while the interphase extends cycle life by suppressing parasitic reactions and ensuring interfacial stability, together underpinning the promising electrochemical performance of SRCE.*" (**Page 15**, **Line 342**)

3. When discussing a novel rational design principle, I believe that another aspect needs to be mentioned as well: Of course, the diluent should not interfere with the solvation structure. However, if a diluent would interact very weakly with the components of the conducting salt phase, macroscopic phase separation would occur. Therefore, some balancing interaction must be preserved. Could the authors comment on the type of interaction that renders the present SRCE miscible?

Response: We thank the reviewer for raising this important point. Indeed, the interaction between the diluent and the conducting salt phase is optimized using Hansen solubility parameters (HSP) to minimize this interaction while still ensuring miscibility of SRCE.

The thermodynamic basis for this miscibility window could be described by HSP. HSP decomposes the total cohesive energy density of a molecule into three independent components, each corresponding to a dominant intermolecular interaction: dispersion (δD), polar (δP), and hydrogen bonding (δH). However, because HSP is strictly defined for neutral molecules, we approximate the HSP of the conductive salt phase using that of DME, the primary Lewis base coordinating Li^+. This approximation is justified on three grounds: (i) DME is the only neutral molecular component in the LiFSI-DME phase; (ii) the diluent-salt phase interaction is dominated by diluent-DME hydrogen bonding, since the ionic clusters are sheathed by DME; and (iii) we use HSP only as a qualitative miscibility criterion, not for absolute thermodynamic prediction. Miscibility is judged by the HSP distance (R_a), calculated as:

$$R_a = \sqrt{4(\delta D_1 - \delta D_2)^2 + (\delta P_1 - \delta P_2)^2 + 4(\delta H_1 - \delta H_2)^2}$$

The data in **Table R2** were obtained from Hansen Solubility Parameters: A User's Handbook and the HSPiP software. Across nine candidate diluents, all miscible cases have Ra < 6 $(MPa)^{1/2}$, while all immiscible cases have Ra > 7 $(MPa)^{1/2}$. As shown in **Table R2** and **R3**, diluent TTE, HFE, OTE, and BTFE achieve miscibility partly through elevated δP (4.0-5.2)

and δH (3.0-4.7). These groups actively engage with FSI^- and DME, thereby modifying the Li^+ solvation structure and perturbing the Li^+-FSI^- interaction. Among the miscible diluents, HFC has the largest and threshold R_a value, which stems from its cyclopentane skeleton (δD=14.3) and its lack of heteroatom coordination sites (δP=2.8 and δH=2.1). In sharp contrast, diluents such as PFP, 1H-Perfluorohexane, Hexane, and Perfluorohexane possess much higher R_a values and are therefore immiscible with the conducting salt phase, showing clear phase separation.

Consequently, the cyclic, saturated, heteroatom-free architecture of HFC positions it right at the edge of the miscibility limitation. This could provide just enough interaction with DME to maintain a single phase, while minimizing perturbation to Li^+, FSI^-, and DME. This dual constraint defines SRCE as a category beyond conventional LHCE, in which the diluent does not merely dilute the HCE but resides within a carefully balanced miscibility window that preserves the Li^+-FSI interaction for inorganic-rich interphase formation.

Table R2. The Hansen solubility parameter values of different solvents/diluents.

Solvent/Diluent	δD $(MPa)^{1/2}$	δP $(MPa)^{1/2}$	δH $(MPa)^{1/2}$	R_a to DME $(MPa)^{1/2}$	Miscible with HCE
DME	15.4	6.3	6.0	-	-
TTE	14.4	5.2	4.7	2.63	Yes
HFE	13.9	5.1	4.0	3.80	Yes
OTE	14.0	4.0	3.5	4.40	Yes
BTFE	13.7	4.4	3.0	4.92	Yes
HFC	14.3	2.8	2.1	5.68	Yes
PFP	12.8	3.7	1.5	7.35	No
1H-Perfluorohexane	12.8	2.1	1.6	8.00	No
Hexane	15.1	0.1	0.1	8.58	No
Perfluorohexane	12.1	1.0	0.4	10.15	No

Note: HFE (1,1,2,2-tetrafluoroethyl 2,2,2-trifluoroethyl ether); OTE (1H,1H,5H-octafluoropentyl-1,1,2,2-tetrafluoroethyl ether). PFP (Perfluoro(2-methyl-3-pentanone)).

Table R3. Optical photographs of different diluents being miscible with HCE.

Diluent	**HFE**	**OTE**	**BTFE**	**HFC**
Miscible with HCE	 Miscible	 Miscible	 Miscible	 Miscible
Diluent	**PFP**	**1H-perfluorohexane**	**Hexane**	**Perfluorohexane**
Miscible with HCE	 Immiscible	 Immiscible	 Immiscible	 Immiscible

Revised Manuscript:

"*By employing nonflammable cyclic fluorinated alkane (1,1,2,2,3,3,4-Heptafluorocyclopentane, HFC) molecules with optimal intermolecular force, i.e., dispersion (δD), polar (δP), and hydrogen bonding (δH), between the diluent and ion pairs. Therefore, the designed diluent could be miscible in HCE and further promote the formation of isolated ionic aggregate nanoclusters (**Figure 1** and **Supplementary Table 1-2**).*" ***(Page 3, Line 82)***

"*Therefore, an optimal R_a could dissociate the interconnections between ion pairs and HFC diluents without inducing phase separation, thereby disassembling the medium-range CIP aggregates network into smaller, isolated nanoclusters.*" **(Page 6, Line 159)**

Further comments:

4. Figures 2a, b & S1 give insights into the interaction strength between Li^+ and DME as well as Li^+ and the diluent, the interaction between DME and the diluent is shown in Figure S6. Because the weakened interaction between diluent and anions in the SRCE is central to the manuscript, I was wondering if additional DFT calculations between FSI^- and TTE as well as

HFC could provide further evidence.

Response: We appreciate the reviewer's insightful suggestion, which directly addresses our key hypothesis. Therefore, we have performed additional Density Functional Theory (DFT) calculations based on the Atoms in Molecules (AIM) theory to explicitly quantify the hydrogen-bonding interactions between the FSI^- anion and the two diluents (TTE and HFC).

Based on the Molecular Dynamics (MD) simulation, the TTE diluent aggressively coordinates with the FSI^- anion through three distinct hydrogen bonds (-33.6, -29.7, and -27.5 kJ mol^{-1}), resulting in a high total hydrogen-bond binding energy of 90.8 kJ/mol (**Figure R13a**). Compared to TTE, the HFC-FSI^- interaction exhibits a substantially weaker affinity, featuring only two hydrogen bonds (-33.0 and -26.5 kJ mol^{-1}) that sum to a remarkably lower total energy of 59.5 kJ mol^{-1} (**Figure R13b**). This pronounced energetic disparity provides direct, compelling atomistic evidence for our core hypothesis. Specifically, owing to its unique cyclic configuration, lower hydrogen polarity, and substantial steric hindrance, the HFC diluent exerts only minimal competing intermolecular forces on the anions, similar to diluent-DME interactions (**Figure R13c** and **d**). The total hydrogen bond energy for diluent-DME/FSI^- interaction is summarized in **Figure R13e**. Consequently, unlike conventional diluents such as TTE and BTFE, HFC exhibits weaker interactions with both FSI^- and DME. This property efficiently mitigates the distortion of the intrinsic Li^+-FSI^- to enable the formation of an inorganic-rich interphase, while promoting phase separation between the diluent and ionic aggregates, thus preserving the isolated solvation nanoclusters.

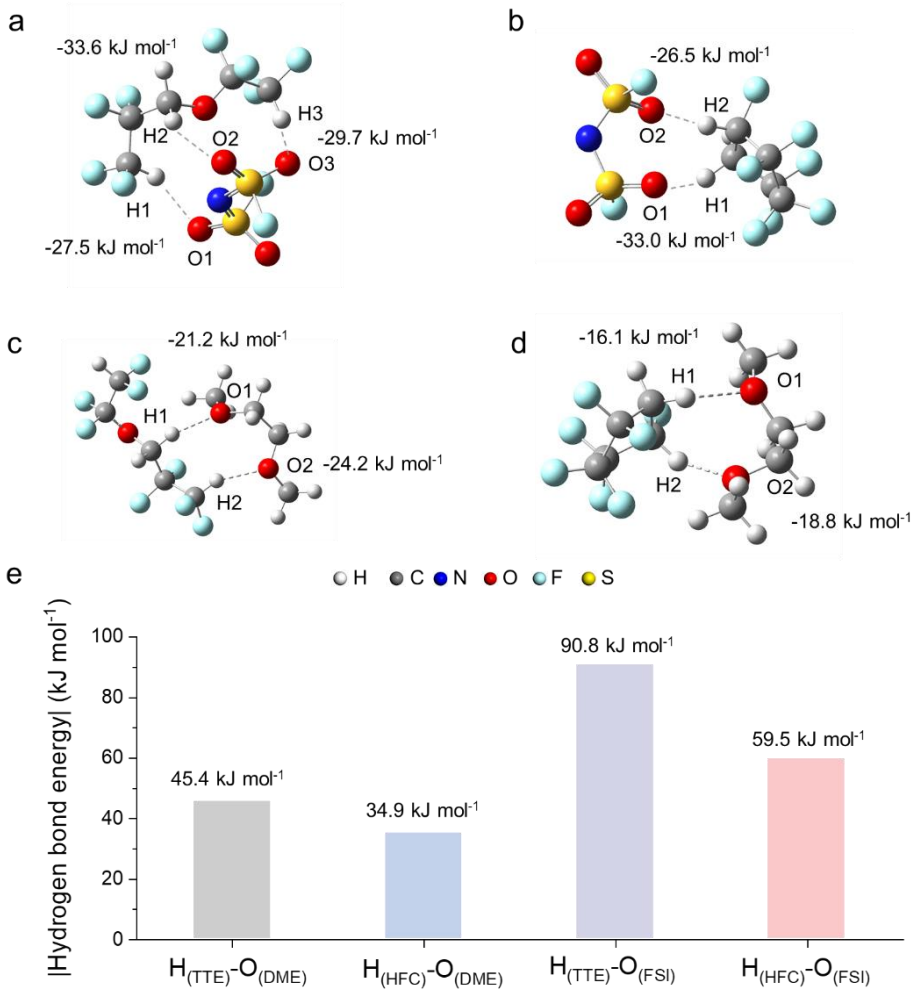

Figure R13. (a-b) Optimized binding configurations and the calculated individual hydrogen-bond energies between the FSI^- anion and the (a) TTE and (b) HFC diluent molecules. (c-d) Optimized binding configurations and the calculated individual hydrogen-bond energies between the DME solvent and the (c) TTE and (d) HFC diluent molecules. (e) Comparison of the total absolute hydrogen-bond binding energies for the respective diluent-solvent and diluent-anion interactions.

Revised Manuscript:

"*Nevertheless, adding TTE diluent into the HCE induces a pronounced upfield shift in the ^{19}F NMR of FSI^- ($\Delta\delta$ = -0.75 ppm), consistent with the density function theory (DFT) calculated hydrogen bond energy, indicating the enhanced electron density around the fluorine atoms due to strong anion-diluent interaction (**Figure 2c**, **Supplementary Figure 3** and **Note 1**). In comparison, the steric hindrance and low polarity of HFC molecules weaken the intermolecular forces interaction with FSI^-, yielding a smaller upfield shift of -0.56 ppm with*

lower bonding energy." (**Page 5**, **Line 120**)

5. Figure S4: Although it is somewhat obvious, the color coding used in the snapshots should be mentioned in the figure caption. Furthermore, I believe that a table with the coordination numbers in the first shell derived from Figure 4d-f would be helpful. This would support statements such as "Consistent with the NMR and MD simulation results, the addition of TTE has a negligible effect on the coordination number of Li^+-FSI- pairs but weakens the inter-CIPs' correlation through strong anion-diluent interactions, resulting in a reduction in both the size and population of nanoclusters.", which is otherwise hard to judge.

Response: We appreciate the reviewer's thoughtful suggestion. We have added the color coding for all atoms in the snapshots within the revised caption of **Supplementary Figure S4** to ensure absolute clarity for readers (**Figure R14**). Furthermore, we have shown the coordination numbers (CNs) in **Table R4** and revised the imprecise expression in the revised **Manuscript** about solvation structure.

As shown in **Table R4**, we have extracted the precise CNs of the first solvation shell (r = 3 Å) from the radial distribution functions. Indeed, the addition of the diluent would interact with DME via hydrogen bonding, competitively displacing solvent molecules from the Li^+ solvation sheath and promoting anion ingress. Therefore, the Li^+-O(DME) coordination number decreases from 2.15 in HCE to 1.70 in LHCE and 1.77 in SRCE, while the Li^+-O(FSI^-) coordination number correspondingly increases from 2.81 to 3.57 and 3.51, consistent with the previous reports[2, 10, 11]. We admire that the statement "the addition of TTE has a negligible effect on the coordination number of Li^+-FSI^- pairs" is absolutely incorrect. This coordination also aligns with the WAXS results. Since the FSI^- still coordinates with Li^+ through its oxygen atoms at similar distances, the high-Q peak at 1.54 $Å^{-1}$ representing the direct cation-anion contact is unvaried in peak position. However, the low-Q peak at 0.94 $Å^{-1}$ is shifted with reduced intensity. This peak originates from medium-range ordered aggregates of CIPs held together by dipole-dipole and other intermolecular forces. The suppression arises because the relatively strong interaction of TTE with FSI and DME weakens the isolation effect of the diluent molecules with a lower HSP distance. Consequently, both the size and the intensity of the CIP aggregation are reduced, but two peaks still remain. We have rephrased this sentence and the associated

discussion in **Figure 2** to acknowledge that introducing either fluorinated diluent measurably replaces DME with FSI^- in the first solvation shell due to the diluent-solvent hydrogen bonding competition. However, the conserved feature between SRCE and HCE is the Li^+ chemical environment (probed by the negligible ^7Li NMR shift, $\Delta\delta$ = -0.007 ppm) and the mesoscale isolation of nanoclusters (probed by WAXS), rather than the first shell composition as our response to **Comment 1**.

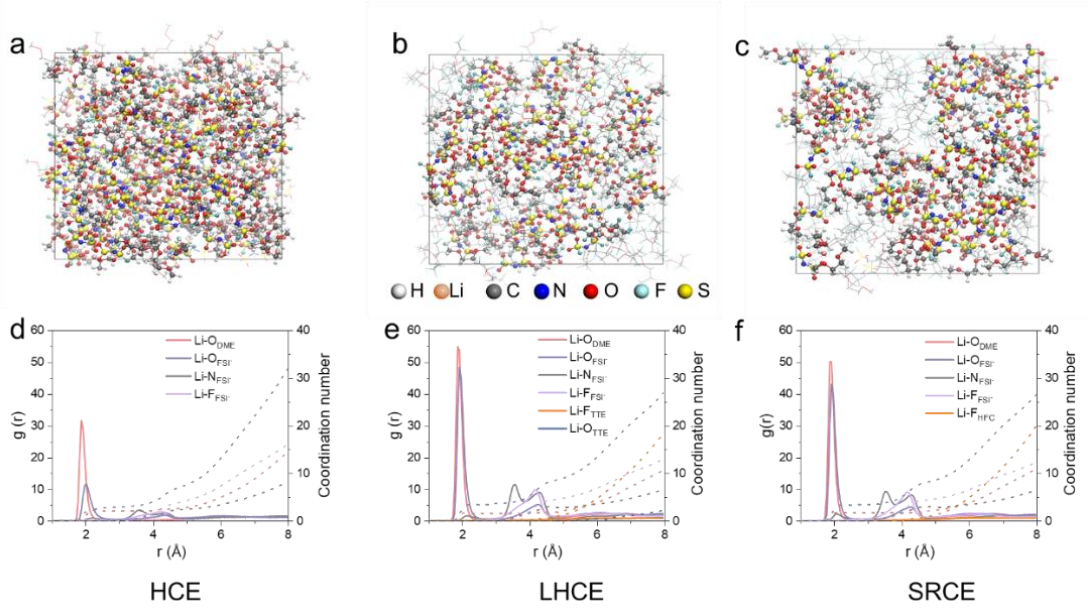

Figure R14. Representative MD snapshots and the corresponding radial distribution functions (RDFs) and coordination numbers (CNs) profiles for (a, d) HCE, (b, e) LHCE, and (c, f) SRCE. Atom color coding in the snapshots: H (white), Li (orange), C (grey), N (blue), O (red), F (cyan), S (yellow).

Table R4. Coordination numbers (CNs) of Li^+ within the first solvation shell (r=3 Å) extracted from molecular dynamics (MD) simulations.

CNs	HCE	LHCE	SRCE
Li-O(DME)	2.15	1.70	1.77
Li-O(FSI^-)	2.81	3.57	3.51
Li-N(FSI^-)	0.10	0.09	0.10
Li-F(FSI^-)	0.06	0.03	0.06

Revised Manuscript:

"*Consistent with the NMR and MD simulation results, the addition of TTE has a remarkable effect on Li^+-FSI^- interactions and the CIPs aggregation peak shifts to a higher Q area with reduced intensity. The slightly stronger interactions of TTE with FSI^- and DME lead to partial but incomplete dissociation of medium-range ionic aggregation, thereby reducing both the size and population of nanoclusters.*" (**Page 6**, **Line 150**)

6. Line 150: Abbreviation HSP is not introduced at this point.

Response: We sincerely thank the reviewer for pointing out this oversight. The abbreviation "HSP" has now been properly introduced with its full name, "Hansen Solubility Parameters", at its first appearance in the main text to ensure clarity for the readers. We have further checked the entire **Manuscript** to ensure that all abbreviations are defined on first use.

Revised Manuscript:

"*...based on Hansen Solubility Parameters (HSP), mutual solubility is governed by...*" (**Page 3**, **Line 72**)

References

1. Wang H, *et al.* Application-driven design of non-aqueous electrolyte solutions through quantification of interfacial reactions in lithium metal batteries. *Nature Nanotechnology* **20**, 1034-1042 (2025).
2. Efaw CM, *et al.* Localized high-concentration electrolytes get more localized through micelle-like structures. *Nature Materials* **22**, 1531-1539 (2023).
3. Yu W, *et al.* Electrochemical formation of bis(fluorosulfonyl)imide-derived solid-electrolyte interphase at Li-metal potential. *Nature Chemistry* **17**, 246-255 (2024).
4. Tan S, *et al.* Additive engineering for robust interphases to stabilize high-Ni layered structures at ultra-high voltage of 4.8 V. *Nature Energy* **7**, 484-494 (2022).
5. Li G-X, *et al.* Enhancing lithium-metal battery longevity through minimized coordinating diluent. *Nature Energy* **9**, 817-827 (2024).
6. Chen X, Zhang Q. Atomic insights into the fundamental interactions in lithium battery

electrolytes. *Accounts of Chemical Research* **53**, 1992-2002 (2020).

7. Zhang N*, et al.* Critical review on low-temperature Li-ion/metal batteries. *Adv Mater* **34**, e2107899 (2022).
8. Ren X*, et al.* Enabling high-voltage lithium-metal batteries under practical conditions. *Joule* **3**, 1662-1676 (2019).
9. Fan X*, et al.* All-temperature batteries enabled by fluorinated electrolytes with non-polar solvents. *Nature Energy* **4**, 882-890 (2019).
10. Cui Z*, et al.* Molecular anchoring of free solvents for high-voltage and high-safety lithium metal batteries. *Nature Communications* **15**, 2033 (2024).
11. Wu Z*, et al.* Deciphering and modulating energetics of solvation structure enables aggressive high-voltage chemistry of Li metal batteries. *Chem* **9**, 650-664 (2023).